We thank reviewer 1 for the helpful comments which helped us to improve the manuscript.

This study explores the effect of radiation on cloud droplet growth in shallow cumulus clouds. Using an offline parcel model it is found that radiative cooling affects droplet growth mostly for drop sizes larger than 10 μm and that the effect is stronger for 3D than for 1D radiation. Recirculating parcel meet several of the criteria that are found to be favorable for a strong effect of radiative cooling on cloud droplet growth and hence contribute more strongly to rain production than if radiative effects on diffusional droplet growth is not taken into account. In a second part, a fully coupled LES simulation with bin microphysics is used to unravel effects of 1D and 3D radiation on the dynamics and the diffusional growth. Although the differences in rain production are overall small, the authors conclude that radiative effects on microphysics increase the rain fraction but that a dynamic evaporation-circulation feedback can decrease rain amount.
The topic of the study is very interesting and relevant for ACP. The manuscript is overall written well and the plots illustrate their content well. However, I have two issue with the study in its present form: First, the authors themselves argue that because in the parcel model raindrops are not allowed to fall out of their parcel, the parcel model is not appropriate to analyze rain formation. Nevertheless parts of their analysis (Fig. 6, 7, 9, 12) focuses on drops of sizes that have considerable fall speed and on rain rate. Second, the differences in the coupled LES simulations are very small. Because simulated precipitation from shallow clouds is such a sensitive variable, I am sceptical that these small differences are robust and due to physical causes rather than random fluctuations due to different realisations. I comment on these two issues in more detail below followed by some specific and technical comments.
---

1) In the method section you argue (and I agree) that the methodology is only valid until the onset of drizzle. Analysing the rain rate (Fig. 12) is therefore not appropriate. In Fig. 6 and 9 the main differences are seen for drops larger than 20 μm radius, which is just the size where cloud droplets turn into drizzle (e.g., Sant et al., 2013, JAS). Even with a less conservative estimate drops with a radius of 40 μm develop considerable fall speed. In the parcel model, those larger drops do not fall out but instead keep on interacting with the smaller drops in their parcel, which is unphysical. Because of the interaction of the large drops with the small droplets, changes in the smaller part of the drop size spectrum are not independent of this issue as soon as some larger drops form.

We agree that the parcel model is an idealized framework where some processes, as e.g. the precipitation formation are not treated in the most realistic way. However, it is a suitable framework for the detailed examination of certain processes. It offers the possibility for a detailed investigation of the differences related to radiation in this study which would be impossible to investigate in an LES. For a more realistic representation of the onset of precip we use the LES in part two of this study.

2) In the coupled LES simulations overall differences are small (e.g., Fig. 14 and 15) and I am wondering whether they are actually causally related to the changes in the radiation. My null-hypothesis would be that the differences in the runs are due to random fluctuations in different realisations. One way to test this is to run an ensemble of simulations for each of the five modifications and analyze whether those ensembles (and their spread) are significantly different from each other.

We agree with the reviewer that the overall differences are small and might not be detectable relative to differences associated with perturbations to thermodynamical inputs in an ensemble of simulations (e.g. Lonitz et al., JAS, 2015). We now state this clearly in the revised manuscript. An ensemble of 3 remembers for the 5 LES runs would require an additional 10 simulations, which would be computationally unfeasible.

Specific comments:

- While I found the rest of the paper well-written and clear, Section 2 was confusing to me. I am not a radiation expert and as other reader might not be either, some improvement is needed here. Please, help the reader by systematically arguing why you need each equation and what it is leading to. E.g., why do you need the forcing term tau and in which equation does it go? On p.5 l.11 you arrive at the same expression you already had on p.3 l.20. Which equation do you use in your model? Also, make sure you explain all variables and constants (see also my technical comment).

Up to equation 6, we essentially follow Harrington et al., 2000. Therefore we summarize only briefly the most important steps/equations. We added some further description and point directly to Harrington et al., 2000 and the necessary equations therein.
From Equation 7 on we describe how the radiative term that is necessary in the droplet growth equation can be derived correctly from the LES model heating rate. We also added further information on why we need these steps and trust that the chapter is more understandable now.

- In the first line of Eq 4, why is there no sum over the different sizes of m within the bin range of bin k? Under which assumptions does the approximation hold? Please use $\approx$ where necessary to indicate the approximation.

This is because for each bin, the equation is solved for the mean mass of the bin, a quantity available in a 2-moment bin scheme but not in typical one moment bin schemes.

- p.6 l.2: Are the trajectories run as tracers that follow the flow or is an average fall velocity of particles size distribution taken into account? From what I read later, I assume they are calculated as tracers of the flow. This would be helpful to specify already here.

The trajectories are run as tracers that go with the flow. We corrected the sentence to: "For the first part of the study 2.7 million Lagrangian air parcel trajectories were recorded in the last two hours of the BOMEX simulation with a 2~second time step."

- How are the cloud droplet size distributions initialized in the offline parcel model?

We use a log-normal distribution. We added this to the manuscript.

- Is the analyzed parcel in Fig 4 and 5 the same? This is not clear from the text.

Yes, both figures show the same parcel. We changed the beginning of the paragraph to the following to be more precise:
"We now take a more detailed look at the same parcel trajectory as shown in (Fig.4). Figure 5 shows this selected parcel which is characterized by moderate vertical velocities..."

- Fig. 7, tau: It would be interesting to calculate the overall contribution to droplet growth for each of the three sizes from the dynamic and the radiative term. The values of the radiative forcing are much smaller than the dynamic terms but the dynamical forcing also has substantial negative contributions.

The overall contribution of the radiative term is positive, while the dynamical forcing undergoes positive and negative terms along this parcel trajectory. Both forcings, however act locally in time as shown in Figure 7.

- p.13 l.8: This sentence is not clear to me: "The radiative cooling does not seem to cause droplet growth in individual parcels beyond the NR case..." Are you saying that in parcels where there are no cloud droplets for NR, also no cloud droplets will grow with 1DR or 3DR?

Yes, this is what we meant. Radiation, acting on droplets itself does not cause additional droplet growth in cases where there was no rain, but strengthens existing droplet growth. However, in a dynamical sense, radiation can cause more rain formation (which is shown later on in the paper).

- Fig 12 and 13: Is this the rain rate at the surface or integrated over all heights? I assume the latter. Please clarify. However, given the restriction of the method to the onset of drizzle, I do not think it is appropriate to analyze the rain rate (see my general comment).

It is vertically integrated. We added this in the manuscript.

- p.16 l.20: How long do the parcels need to be in an environment with qc less than 0.01 g/kg to be called a recirculation? Do your statistics substantially change if you increase or decrease a threshold in time a bit?

We did not apply a threshold in time for the analysis, only for qc.
However, we did perform a “back of the envelope” calculation. Setting upper and lower thresholds in space (e.g. 50m or 200m for the “near cloud” environment) and speed (0.5m/s to 5 m/s), a time period for a parcel (if it travels straight back and forth) would be between 20s and 13min. Our parcels are within this range (see histogram at the end of this text, which we also added to the manuscript, now Figure 13).
Setting an upper limit in time (e.g. 5min, which is more than 90% of our recirculating parcels), the changes in our results are very small. The maximum contribution of the rain rate 58% reduces to 56%. For a time threshold of 2min, the maximum reduces to 45%. We

added this analysis to the manuscript, too. For comparison, the second figure (similar to Fig. 14 in the paper) at the end of this text shows the rain rate for the 2min threshold.

- To quantify how much recirculation parcels contribute, I think it makes more sense to normalize by the total rain rate for each simulation, e.g., RR_1DR_recirculating/RR_1DR_total. Otherwise you combine the effect of radiation and recirculation.

This is a valuable comment. However, as our study is not purely focused on the effect of recirculation, but also includes the radiative effects, we prefer to show the figure as is. The change due to recirculation only is very much the same for the three cases (NR, 1D RAD and 3D RAD) and about 30%. We now mention this in the text as follows: "The amount of the rain rate due to recirculation (when normalized to each of our simulations and therefore without considering radiative effects) is about 30% in our study."

- p.18 l.9 and elsewhere: Please do not use "significant" when you did not test for significance. "considerable" or "substantial" might be alternatives.

Corrected.

- Fig. 14,15,18: Why don't you combine those three figures into one? If I am not mistaken you just need to add one line in Fig. 14. It would allow the reader to compare simulation pairs, which the manuscript does not focus on. Also, I do not see the advantage of comparing different time periods for the different simulations in Fig. 17 and 19. If the results are robust, I would expect the results to be qualitatively the same for other time periods. Then Fig. 17 and 19 could be combined and show all five simulations. Also, show all five simulations in Fig. 16.

Thank you for this comment. We do have reasons why we show the figure as they are, which are the following:

a) We want to point out different effects. This is why we show Figure 14, 15 and 18 the way they are. First, we only focus on thermal radiative effect on the droplet growth itself, not focusing on dynamical feedbacks (Figure 14 and Section 4.3.1). Second, we want to show the effect of 3D thermal radiation on dynamics and on microphysics (Figure 15 and Section 4.3.2). Finally, we separate 1D and 3D thermal radiative effects (Figure 18 and Section 4.3.3).

b) The different time periods are chosen, because they focus on specific/detailed developments within the simulations. In the case where we compare 3D radiative effects on microphysics and dynamics, an increase in rain arises roughly around 7 hours, therefore we expect changes in the variables related to the specific dynamics at this time (which is shown). The same reason applies to Figure 19. When comparing 1D and 3D thermal radiation, differences in both simulation occur at different time periods.

- Section 4: If the results turn out to be robust (see my general comment), my interpretation here would be that applying radiative cooling to microphysics leads to larger cloud droplets and drizzle drops especially at the cloud edges, which then can lead to two opposing effect: 1) The larger drops re-enter the cloud and have a better chance to form rain than if they had not grown by radiation. Therefore rain formation is en-

hanced. 2) The larger drops decrease evaporation at the cloud edge, which via the evaporation-circulation feedback leads to weaker updrafts and hence less rain formation. Going from 1DD to 1DD_1DM effect 1 seems to dominate; going from 3DD to 3DD_3DM effect 2 seems to dominate. If you agree with this interpretation, I think it would be worth to make this opposing effects clearer in the manuscript. Here, it would strengthen your point if you analyze the evaporation rates for all simulations (Fig. 16). Also, I suggest to contrast the difference in evaporative cooling at the cloud edge with the difference in radiative cooling rates at cloud edge to unravel whether a decrease in evaporative cooling or the increase in radiative cooling dominates if you go from 1DD to 3DD_3DM.

Thank you for summarizing this. We revisited the summary section and made these points clearer.

- p.1 l.11 "Small amounts of rain are ..." and p. 24 l.12 "... rain covers a larger area": I do not see that these sentences are true for 3DD to 3DD_3DM (Fig. 14).

When looking at the surface precipitation fraction (Fig. 15, second from top) the area covered by rain is slightly larger in the 3DD_3DM case compared to the 3DD case. The differences are small though, but visible throughout the simulation time until the dynamical effects dominate.

Technical comments:

- Please check the standards of the journal. Usually references should be ordered by year (e.g., p.3 l.6 or l.10, check elsewhere) and brackets in brackets are not allowed.

Corrected.

- pay attention if you place variables (math mode) in the text, e.g., T_inf on p.3 l.17 or q on l.27

Corrected.

- make sure to explain all variables and constants, e.g., D and e_s on p.3 l.28 or t_f on p.4 l.13

Corrected.

- p.6 l.7: Harrington et al. (2000)

Corrected.

- caption Fig.4: where there parcel stays -> where the parcel stays

---

Corrected.

- Fig 4: What the color scale of qc in b-d? It seems not the be the same as for the trajectory in a.

Figure 4 b-c only shows the trajectory itself, not colored by qc or any other variable. We added this to the caption.

- p.11 l.4: four -> three

Corrected.

- p.12 l.12: the the -> the

Corrected.

- p.18 l.24: stronger stronger -> stronger

Corrected.

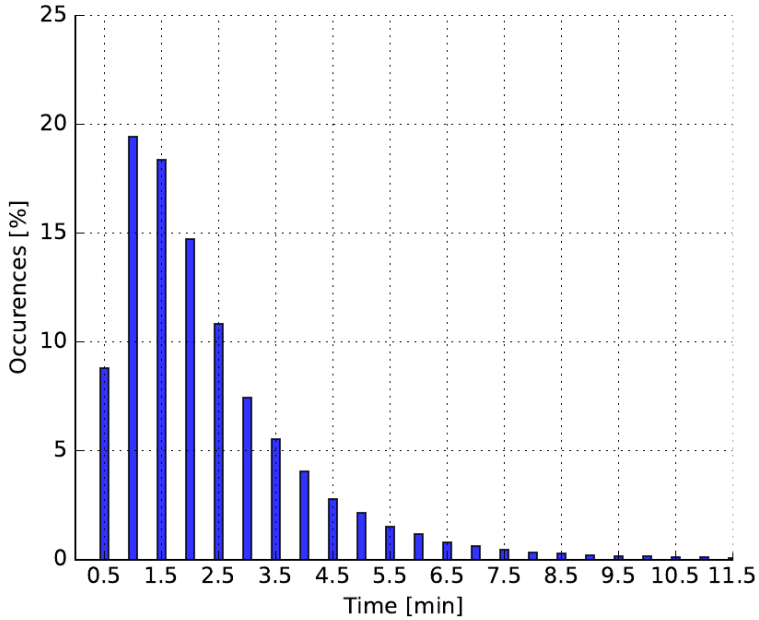

Histogram of recirculation times.

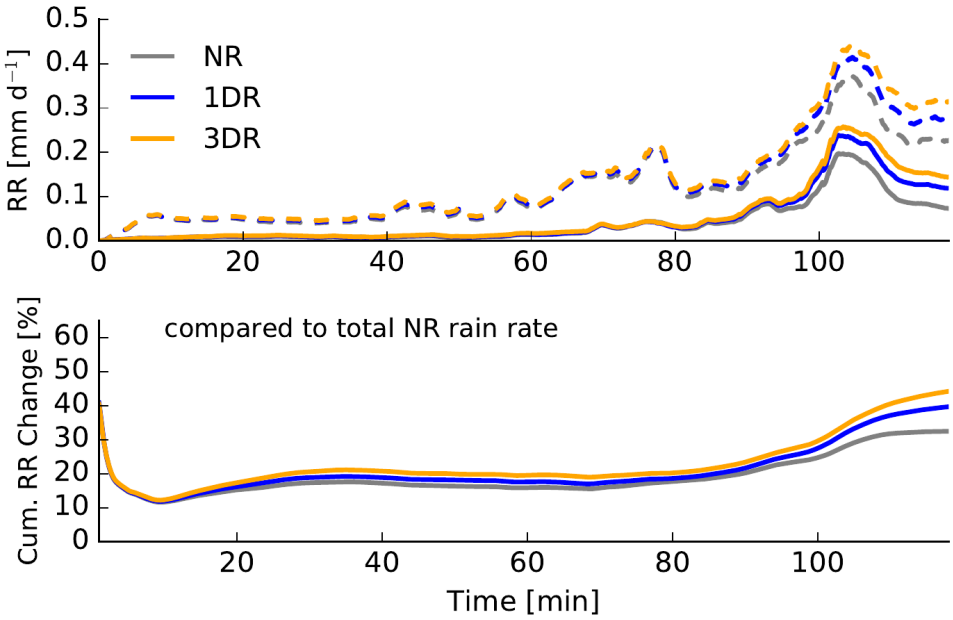

Rain rate calculated from the parcel ensemble (dashed) and from recirculating parcels (solid) applying a qc threshold of 0.01 g/kg and a time threshold for recirculation events of 2min.

We thank reviewer 2 for the helpful comments which helped us to improve the manuscript.

I support publication. The manuscript is quite well written as it is. There are a few relatively minor points that the authors may wish to consider that I have raised below, but, overall, the manuscript is in good shape.
It seems the question as to why cloud droplet spectra are “broad” has been plaguing the cloud physics community since we were first able to compare measured droplet distributions with calculations of adiabatic growth. There are many competing hypotheses as to why this discrepancy exists, which the authors have referenced in their introduction. In my opinion, one reason that we may have been puzzled about this for so long is that there’s no single reason for this spectral broadening, and in most cases, it is probably a combination of factors. Radiative effects certainly play some role, and this paper shows some of the effects for shallow cumulus clouds.
---

pg. 1, last line: “Smaller droplet sizes reflect more radiation back to space...” Clarify please. Perhaps just add that this is true if the liquid water is held constant.

Thank you! We added: "for constant liquid water".

References to Pruppacher and Klett: This is a 700 page book. At least reference the chapter for the point you are trying to make.

Chapter 14, pages 569-616, is added to the citation.

Pg. 2; line 1: “...larger droplets allow radiation to settle more easily...” Settle implies that gravity is the driving force. I think that you mean that radiation penetrates to the surface more easily when the droplets are larger.

Thank you for pointing this out. We changed "settle" to "penetrate".

Pg. 3, line 5: You reference high local cooling rates for cumulus clouds in the context of the finite size. It would be useful to provide a value for typical cooling rates for stratus clouds at cloud top.

A comparison to stratus clouds in this context is difficult. Heating rates depend amongst other things on the temperature profile, liquid water content or, as they are volume quantities also on the grid box size of a simulation. But we see your point that some clarification for 1D and 3D radiative transfer cases is necessary. The already cited literature (and a new publication) compare heating rates in 3D and 1D in the same cloud fields based on the same background atmosphere and resolution.
We added: "Klinger and Mayer (2016, their Figure 11) showed that local peak differences in cooling rates between 1D and 3D thermal radiation in cumulus cloud fields can reach 20-120%, depending on the cloud field resolution. But the differences between 1D and 3D thermal radiation are not only focused on local grid boxes. Kablick et al. (2011) and Crnivec and Mayer (2019) showed that layer averaged 1D and 3D heating and cooling differences can be up to 1’K/d, which is the same order of magnitude as clear sky cooling."

Pg. 6, line 15: Check the parentheses on the reference to Harrington.

Checked.

Pg. 7, line 6: The first two sentences are redundant. One or the other is fine.

Corrected.

Pg. 12, line 12: Two consecutive occurrences of “the”.

Corrected.

Pg. 18, line 24: Two consecutive occurrences of “stronger”.

Corrected.

Pg. 17 (last line) continuing to first lines of pg. 18: In the discussion of Figure 14, the statement is made that the rain water path shows an increase an hour after restart for the 3DD 3DM case. Is that a significant difference? I can see that the line is slightly higher than the other three, but the difference disappears after time 6.5. In the text, that’s attributed to noise, but then why isn’t the initial increase just noise as well?

We agree that the word “noise” is misleading and have reworded the text accordingly.

Cloud Droplet Growth in Shallow Cumulus Clouds Considering 1D and 3D Thermal Radiative Effects

Carolin Klinger[1,2], Graham Feingold[1], and Takanobu Yamaguchi[1,3]

[1]Chemical Sciences Division, NOAA Earth System Research Laboratory (ESRL), Boulder, Colorado, USA
[2]Ludwig-Maximilians-Universität München, Lehrstuhl für Experimentelle Meteorologie
[3]Cooperative Institute for Research in Environmental Sciences, University of Colorado, Boulder, Boulder, CO, USA

Correspondence: Carolin Klinger (carolin.klinger@physik.lmu.de)

Abstract. The effect of 1D and 3D thermal radiation on cloud droplet growth in shallow cumulus clouds is investigated using large eddy simulations with size resolved cloud microphysics. A two step approach is used for separating microphysical effects from dynamical feedbacks. In step one, an offline parcel model with bin resolved microphysics is used where cloud droplets are grown along previously recorded Lagrangian trajectories. It is shown that thermal heating and cooling rates can enhance droplet growth and rain production. Droplets grow to larger size bins in the 10-30 μm radius range. The main effect in terms of rain production arises from recirculating parcels, where a small number of droplets is exposed to strong thermal cooling at cloud edge. These recirculating parcels, comprising about 6-7% of all parcels investigated, make up 45% of the accumulated rain rate for the no radiation simulation and up to 60% when 3D radiative effects are considered. The effect of 3D thermal radiation on rain production is stronger than that of 1D thermal radiation. 3D thermal radiation can enhance the rain rate up to 40% compared to standard droplet growth without radiative effects in this idealized framework.

In the second stage, fully coupled large eddy simulations show that dynamical effects are stronger than microphysical effects, as far as the production of rain is concerned. 3D thermal radiative effects again exceed 1D thermal radiative effects. Small amounts of rain are produced in more clouds (over a larger area of the domain) when thermal radiation is applied to microphysics. The dynamical feedback is shown to be an enhanced cloud circulation with stronger subsiding shells at the cloud edges due to thermal cooling, and stronger updraft velocities in the cloud center. It is shown that an evaporation-circulation feedback reduces the amount of rain produced in simulations where 3D thermal radiation is applied to microphysics and dynamics, in comparison where 3D thermal radiation is only applied to dynamics.

1 Introduction

Cloud droplets form in saturated environments by condensation of water vapor on cloud condensation nuclei (CCN). In the first phase of the droplet's lifetime, cloud droplet growth follows Köhler theory (Köhler, 1936). If a certain critical radius is reached a droplet can grow further, following diffusional droplet growth theory. From a certain droplet size onward, rain formation processes such as collision and coalescence dominate growth (Pruppacher and Klett, 2010).

The droplet size distribution in clouds has important implications for the Earth's atmosphere. The size distribution of droplets determines how much solar radiation is reflected back to space. Smaller droplet sizes reflect more radiation back to space (for

constant liquid water), thus leading to a cooling of the atmosphere while larger droplets allow radiation to ~~settle~~ penetrate more easily to the surface, thus allowing more radiation to be absorbed ~~(Ramanathan et al., 1989; Boucher et al., 2013; Stephens, 2005).~~ (Ramanathan et al., 1989; Stephens, 2005; Boucher et al., 2013). Furthermore, the droplet size distribution determines the formation of rain in clouds. Droplets that reach the 10 - 30 μm radius range can lead to rain formation. Only very small numbers of droplets of this size (order 1 per liter) are necessary to initiate the process of collision and coalescence. It is known that a broad droplet size spectrum is necessary for these processes to start, however cloud droplet growth in the diffusional growth theory slows down when droplets reach 10 μm and collision and coalescence is not yet effective (the so called collision-coalescence bottleneck Simpson (1941); Langmuir (1948); Mason (1960); Pruppacher and Klett (2010)). Different processes can cause broadening of the droplet size spectra, e.g. turbulence (Grabowski and Wang, 2013), the associated supersaturation fluctuations ~~(Shaw et al., 1998; Cooper, 1989; Lasher-Trapp et al., 2005; Grabowski and Abade, 2017)~~(Cooper, 1989; Shaw et al., 1998; Lasher-Trapp giant CCN (Feingold et al., 1999; Cheng et al., 2009) and radiation (Harrington et al., 2000; de Lozar and Muessle, 2016). As soon as rain is initiated, the cloud system morphology and intrinsic properties can change as the dynamics of the system change.

Radiative effects on cloud droplet growth have been studied in various ways in the past. Among the earliest are the studies by Roach (1976) and Barkstrom (1978). Both analyzed the growth of an individual droplet and showed that droplets can grow to 20 μm and larger by radiative cooling, even in a subsaturated environment. Guzzi and Rizzi (1980) and Austin et al. (1995) took the next step and looked at the effect of radiation on the growth of a droplet population. Guzzi and Rizzi (1980) showed increased droplet growth in the diffusional droplet growth regime, while Austin et al. (1995) also included ~~collision-coalesence~~ collision-coalescence and found earlier onset of rain by a factor of 4. An important issue of the application of radiation to droplet growth is the time scale of the temperature exchange. Davies (1985) estimated the time until droplets reach a steady state in temperature exchange. For most droplet sizes, the time scale was small enough to make the assumption of a steady state system feasible. Bott et al. (1990) simulated radiative fog, thus including microphysical and dynamical feedbacks. The inclusion of the radiative term in the droplet growth equation had important consequences for the lifetime of fog. The enhanced growth of larger droplets by radiation and associated gravitational settling caused a reduction of liquid water in the fog. The oscillation of liquid water (in periods of 15-20 min) could only be simulated by including radiative effects. Ackerman et al. (1995) simulated stratocumulus clouds, using a bin microphysical model including 1D radiation. The stronger diffusional growth in the simulations with radiative effects reduced supersaturation and therefore the number of small droplets. The reduced number of droplets and the larger droplet size resulted in more drizzle and therefore a lower cloud optical thickness. Observations of nocturnal stratocumulus were remodeled with Lagrangian parcels by Caughey and Kitchen (1984). They stated that: 'A simple Lagrangian model suggested that the larger drops grew within the zone of high net radiative loss around cloud top'. Harrington et al. (2000) used a LES and an independent parcel model, including bin microphysics and radiative effects on droplet growth. They showed that only parcel trajectories spending long periods of time at cloud top (10 minutes or more), can cause the droplet size spectrum to broaden via radiative cooling. They also found an earlier onset of drizzle production, however, this occurred along parcels that would produce drizzle anyhow. They concluded that radiative cooling may reduce the time for drizzle onset. The recent theoretical study of Brewster (2015) and direct numerical simulations by de Lozar and

Muessle (2016) re-emphasize the hypothesis that thermal radiation might influence droplet growth significantly and lead to a broadening of the droplet size spectra and thus enhance the formation of precipitation. Similarly, Zeng (2018) investigated the effect of thermal radiation on rain formation in a precipitating shallow cumulus case and found broadening of the droplet size spectrum and earlier rain formation.

In this study, we investigate the role of thermal radiation on cloud droplet growth in cumulus clouds. The limited lifetime of cumulus clouds changes the radiative impact compared to former studies where stratiform clouds where investigated. The finite size of the cumulus clouds and the high local cooling rates of several hundred K/d at cloud top and at cloud sides (e.g. ~~Klinger and Mayer (2014); Klinger et al. (2017); Kablick et al. (2011)~~Kablick et al. (2011); Klinger and Mayer (2014); Klinger et al. (201 suggest that the investigation of 3D thermal radiation effects might have a significant effect on drop growth. ~~Whether this stronger~~ Klinger and Mayer (2016) (their Figure 11) showed that local peak differences in cooling rates between 1D and 3D thermal radiation in cumulus cloud fields can reach 20 - 120%, depending on the cloud field resolution. But the differences between 1D and 3D thermal radiation are not only focused on local grid boxes. Kablick et al. (2011) and Črnivec and Mayer (2019) showed that layer averaged 1D and 3D heating and cooling differences can be up to 1 K/d, which is the same order of magnitude as clear sky cooling. Whether the stronger local 3D cooling affects droplet growth compared to 1D thermal cooling and, if cooling in general causes changes in droplet growth in cumulus clouds are questions addressed in this study. The focus of this work is on thermal radiative effects on droplet growth. At the end of the study, we will briefly investigate thermal radiative effects on dynamics as e.g. shown by ~~Klinger et al. (2017), Guan et al. (1995, 1997)or Mechem et al. (2008)~~ Guan et al. (1995, 1997), Mechem et al. (2008) or Klinger et al. (2017).

The paper is structured as follows: Section 2 provides the necessary theory, section 3 the model setup. Section 4 analyses the results of our study. Summary, conclusion and outlook are provided in Section 5.

2 Theory

The energy budget at a droplet surface is described by Eq.(1) which combines water vapor diffusion to the droplet and latent heat release, where l_v is the latent heat, $dmdt^{-1}$ the change in mass (m) over time (t), r the droplet radius, K the thermal diffusivity and ~~T_d and T_{inf}~~ T_d and T_inf the droplet temperature and the temperature of the surrounding air:

$$l_v \frac{dm}{dt} = 4\,\pi\,r\,K\,(T_d - T_\mathrm{inf}). \tag{1}$$

Following Roach (1976), the equation can be extended by a radiative term (Eq. (2)), where $HR_\lambda(r) = 4\pi r^2 q_{abs,\lambda}(r) F_{net,\lambda}(r)$ is the emitted or absorbed power of an individual droplet. $q_{abs,\lambda}(r)$ is the absorption efficiency per droplet radius ~~(r)~~ and wavelength (λ) and $F_{net,\lambda}(r)$ the net radiative gain/loss of a droplet per radius and wavelength in W/m^2.

$$l_v \frac{dm}{dt} = 4\,\pi\,r\,K\,(T_d - T_\mathrm{inf}) + \int_\lambda HR_\lambda(r)\,d\lambda \tag{2}$$

Harrington et al. (2000) transformed the equation to the notation of the bin microphysical model of Tzivion et al. (1989). We will follow their notation in the following, as we use the same bin microphysical model. Thus, Eq. (2) becomes

$$\frac{dm}{dt} = C(P,T)\,\frac{m^{2/3}}{m^{1/3}+l_0}\left[\eta(t) + J(P,T)\,m^{1/3}\,HR(m)\right] \tag{3}$$

where l_0 is a length scale representing gas kinetic effects, $\eta(t)$ the excess specific humidity (~~q_v-$q_s(T)$~~q_v-$q_s(T)$) and $C(P,T) = \frac{4\pi}{Cr_s}$; $C = \frac{R_v T_{\inf}}{De_s(T_{\inf})} + \frac{l_v}{T_{\inf} K}\left(\frac{l_v}{R_v T_{\inf}} - 1\right)$ where D is the diffusion coefficient, R_v is the specific gas constant and e_s is the saturation vapor pressure . $J(P,T)$ summarizes constants concerning the radiative term: $J(P,T)=\frac{r_s l_v \alpha_c}{K R_v T}$ with r_s the saturation mixing ratio, $\alpha_c=\left[\frac{3}{4\pi\rho_l}\right]^{\frac{1}{3}}$, ρ_l the liquid water density and R_v the gas constant of moist air.

$HR(m)$ of a droplet is the wavelength band (i) integrated radiative gain or loss, weighted by the absorption efficiency ~~,~~ ~~transformed to~~ for a mass size-bin (k) for the bin microphysical model. Harrington et al. (2000) showed that ~~for~~ the radiative term $HR(m)$ can be approximated with the mean mass ($\overline{m}_k$) of a drop size bin k~~, $HR(m)$ can be approximated with:~~ :

$$HR(m) = \sum_{i}^{N_{bands}} q_{abs,i}(m)\,F_{net,i} \approx \sum_{i}^{N_{bands}} \overline{q}_{abs,i}(\overline{m}_k)\,F_{net,i} = HR(\overline{m}_k) \tag{4}$$

This radiative term must be included in the equation for supersaturation and for droplet growth. The equation for the supersaturation, ~~including radiative terms~~ in our case water vapor excess η, is:

$$\frac{d\eta}{dt} = D - A(P,T)\,\frac{dM}{dt} \tag{5}$$

where the function $A(P,T)$ connects the integrated mass growth rate $dM\,dt^{-1}$ to changes in η. Including the integrated radiative terms of the mass growth rate $\mathcal{R}$, Eq. 5 becomes

$$\eta(t) = \left\{\left[\eta(t_0) - \frac{D}{G}\right]e^{-G(t-t_0)} + \frac{D}{G}\right\} - \frac{\mathcal{R}}{G}\left[1 - e^{-G(t-t_0)}\right] \tag{6}$$

where D represents the increase/decrease in η due to dynamics, G is the contribution to η from the standard droplet growth and $\mathcal{R}$ the contribution to η from radiatively driven droplet growth. Here it can be seen that the additional radiative term can increase/decrease η due to radiative heating/cooling. For a more detailed explanation the reader is referred to Harrington et al. (2000), their Equations 6 - 10.

For solving the condensation equation in the two-moment framework of Tzivion et al. (1989), where both mass and number in a bin k are predicted, Eq. (3) has to be integrated ~~in time~~ over one time step from t_0 until t_f. Again, we follow Harrington et al.

(2000) to calculate the forcing τ (the gain or loss of mass of a droplet) of the droplet growth equation:

$$\int_{m_o}^{m_f} \frac{m^{1/3} + l_o}{m^{2/3}} =$$

$$C(P,T) \int_{t_0}^{t_f} \eta(t)\, dt \; + \; \overline{m}_k^{(1/3)}\, C(P,T)\, J(P,T)\, HR(\overline{m}_k)\, \Delta t =$$

$$\tau_d + \tau_r = \tau \tag{7}$$

where τ is the combined dynamic (τ_d) and radiative (τ_r) forcing of the droplet growth equation and m_0 and m_f are the initial and final mass of the droplet before and after condensation/evaporation.

While What remains now is how the radiative term $F_{net,\lambda}(r)$ in Eq. 2 is derived from the radiation scheme in the LES model. Heating rates in LES models are calculated spectrally from bulk water. These heating rates include contributions from liquid water/cloud water as well as water vapor and other atmospheric gases. Former studies, e.g. Roach (1976) and Harrington et al. (2000), used a 1D radiative transfer approximation and calculated the individual droplet absorption and emission from the upwelling and downwelling fluxes, we . We, however, include 3D-radiative effects. Our 3D radiative transfer approximation is designed to provide 3D heating rates. We estimate the individual droplet emission/absorption from a volume heating rate by separating and therefore have to separate the heating/cooling from the liquid water phase (HR_{liquid}) from the total heating/cooling (from liquid water and atmospheric gases, HR_{tot}). We follow the approach of Mayer and Madronich (2004) which showed the relationship between heating/cooling rates and the actinic flux F_0 to be :

$$HR_{tot,\lambda} = -k_{abs,\lambda} F_0$$

$$HR_{tot,\lambda} = -k_{abs,\lambda} F_0 \;\; HR_{liquid,\lambda} = -k_{abs,liquid,\lambda} F_0 \tag{8}$$

where k_{abs} is the absorption coefficienttotal absorption coefficient and $k_{abs,liquid}$ the absorption coefficient of liquid water. It therefore Combining these two equations into each other it follows that the heating/cooling rate resulting from the liquid water absorption is:

$$HR_{liquid,\lambda} = -\frac{k_{abs,liquid,\lambda}}{k_{abs,\lambda}} HR_{tot,\lambda}. \tag{9}$$

This total heating rate now has to be distributed amongst all droplets in the volume. The total heating or cooling from the liquid water of a grid box (for a single wavelength λ or wavelength band i) is the sum of all droplet contributions to the heating or cooling

$$HR_{liquid,\lambda} = \int n(r) h_\lambda(r) dr \tag{10}$$

where $n(r)$ is the number of droplets of radius r per radius interval dr and $h_\lambda(r) = 4\pi r^2 q_{abs,\lambda}(r) F_{net,\lambda}(r)$ the heating or cooling rate of each droplet at radius r with the absorption efficiency $q_{abs,\lambda}(r)$ and the net-heating of each droplet $F_{net,\lambda}(r)$. Assuming steady state (e.g. ~~(Davies, 1985)~~Davies (1985)), $HR_{liquid,\lambda}$ is equally distributed among all droplets and the individual ~~droplet~~ heating or cooling ($F_{net,\lambda}(r)$) ~~is therefore~~

~~$$F_{net,\lambda}(r) = \frac{HR_{liquid,\lambda}}{\int 4\pi r^2 n(r) q_{abs,\lambda}(r) dr}$$~~

~~and our radiative term~~ of a droplet of size r in Eq. (2) ~~becomes $4\pi r^2 q_{abs,\lambda}(r) F_{net,\lambda}(r)$~~is therefore

$$F_{net,\lambda}(r) = \frac{HR_{liquid,\lambda}}{\int 4\pi r^2 n(r) q_{abs,\lambda}(r) dr} \tag{11}$$

.

3 Methodology

To estimate the effect of 1D and 3D thermal radiation on cloud droplet growth we use a two-stage approach. First, to estimate the impact of thermal radiation on droplet growth and to gain insight into physical processes, we use Lagrangian parcels (Yamaguchi and Randall, 2012) recorded during a LES simulation (System for Atmospheric Modelling, SAM; ~~(Khairoutdinov and Randall, 2003~~ with the bin emulating two moment bulk scheme of Feingold et al. (1998). These parcel trajectories are then used to drive an independent (offline) parcel model including a bin microphysics scheme (Tzivion et al., 1987; Feingold et al., 1999). (The disparity between LES and parcel model microphysics schemes is of no consequence because the parcel model simulations are non-interactive.) We separate between 1D (RRTMG, ~~(Mlawer et al., 1997; Iacono et al., 2000)~~Mlawer et al. (1997); Iacono et al. (2000), 1DR) and 3D thermal (~~(Klinger and Mayer, 2016)~~Klinger and Mayer (2016), 3DR) radiative effects and compare both results to the droplet growth without radiative impacts (NR) and to each other. This approach allows us to focus on the effect of thermal radiation on droplet growth, without the interaction of changing dynamics that would occur in a fully coupled LES simulation. Second, we ran a fully coupled LES simulation with the TAU bin-microphysics scheme (Tzivion et al., 1987; Feingold et al., 1988; Tzivion et al., 1989), where 1D and 3D thermal radiative effects (heating rates) are applied to the droplet growth, and to the dynamics, or to just one of the two. We chose a shallow cumulus case with weak precipitation (BOMEX) where we expect the effects of thermal radiation on cloud droplet growth to be tangible, and not overwhelmed by the rapid development of precipitation encountered in deeper trade-wind cumulus environments. We expect that it would be harder to discern these effects in a more strongly precipitating case.

In both cases the simulations were run with 75 m horizontal and 50 m vertical resolution for a 45x45 km^2 domain. The simulations for the trajectories were run for 6 hours in total; the last 2 hours are used for evaluation. The coupled LES cases were run for 8 hours in total.

For the first part of the study 2.7 million Lagrangian air parcel trajectories were recorded in the last two hours of the BOMEX

simulation with a 2 second time step. The simulation was driven by 1D thermal radiation, but we recorded 3D thermal radiation along the same parcels. This allows us to compare the same parcels, driven by the same variables (liquid water potential temperature, pressure, vertical velocity) in the later part of the study. The difference in the results of the independent parcel model ensemble is therefore only due to the difference in the 1D and 3D thermal heating/cooling rates and their impact on cloud droplet growth. Changes to the approach of ~~(Harrington et al., 2000)~~ Harrington et al. (2000) were explained in Section 2. The total number of aerosol particles (assumed to be ammonium sulfate) is 100 cm^{-3} with a median radius of 0.1 μm and a geometric standard deviation of 1.5 ~~.~~ (log-normal distribution). The bin model includes diffusional growth and the growth by collision and coalescence and covers 36 size bins with a mass doubling from one bin to the next.The radius of the first bin (lower bound) is 1.56 μm. Aerosol particles are activated based on the locally calculated supersaturation, and placed in the first bin. We neglect solute- and kelvin-effect in this framework, because they have a minor impact for $r > 1.56$ μm. Kinetic and ventilation effects are taken into account.

With the parcel model approach, we focus on the effects of thermal radiation on microphysics, neglecting any changes in cloud development that would occur due to feedbacks within a LES framework. A further advantage of this method is that spurious spectral broadening due to advection is avoided ~~Harrington et al. (2000)~~(Harrington et al., 2000). Limitations of this method are, e.g., that the drizzle process is not described as all droplets follow the parcel trajectory, the liquid water content (~~q$_c$~~q_c) is not reduced as the parcels do not 'rain out' and radiation does not change along the parcel trajectories when the size distribution (or ~~q$_c$~~q_c) changes. The method is thus mostly useful for examining the *onset* of drizzle. Nevertheless, the goal is to examine the combined effect of droplet growth and thermal radiation with and without the radiative effects in a framework that allows for realistic fluctuations in q_c bearing in mind that rain formation is treated in an idealized way. In the subsequent section LES will be used for a more realstic treatment of these processes.

As the microphysical schemes in our LES simulation and in the offline parcel model are different (2 moment bulk vs. bin), small differences in the predicted liquid water can occur. Therefore, the calculated heating/cooling rates of the LES might occasionally be too high for the application in the parcel model, thus causing unrealistic droplet growth. We therefore ~~applyed~~ applied a threshold to the cooling. Whenever the distributed droplet cooling (~~F$_{net}$~~F_{net}) was larger than the black body emission ($\sigma T^4/6$; the factor 1/6 accounting for the window regions and emission to only one hemispheric dimension) the cooling of the droplet was set to the black body emission value. Tests showed that the discrepancy between the liquid water content of the parcel model and the LES occurs most often at the edges of clouds where ~~q$_c$~~ q_c is very small. In this area, droplet cooling can be regarded as "black", because droplets are exposed to clear sky.

The coupled LES simulation have a similar setup, but we used the bin-microphysics scheme from the beginning of the simulation. We restarted after 4 hours from a base simulation with 1D thermal radiation passed to dynamics only. We separate 5 cases:

- 1D thermal radiation applied to dynamics only ($1DD$)
- 1D thermal radiation applied to dynamics and droplet growth ($1DD\_1DM$)
- 3D thermal radiation applied to dynamics only ($3DD$)

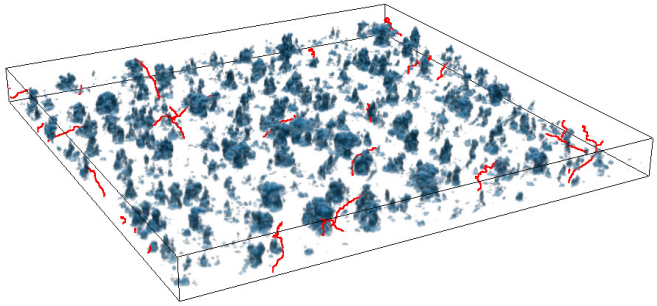

Figure 1. Time snapshot of the BOMEX shallow cumulus cloud field. Displayed is ~~q_c~~ q_c and selected parcel trajectories (red).

- 3D thermal radiation applied to dynamics and droplet growth ($3DD\_3DM$)
- 1D thermal radiation applied to dynamics and 3D radiation applied to droplet growth ($1DD\_3DM$)

These five simulations allow us to a) look at the effect of thermal radiation on droplet growth, b) separate between 1D and 3D thermal radiative effects and c) to separate the droplet growth effect from dynamical effects.

4 Simulations Results

4.1 Parcel Model - Cloud Field Statistics and Properties

~~A time snapshot of the cloud field with some selected parcel trajectories is shown in Fig. **??**. This figure~~ Figure 1 shows a time snapshot of the cumulus field and selected time-dependent trajectories (red). From our 2.7 million parcel trajectories we selected about 340,000 that make contact with a cloud for further investigation. This number was chosen as it ~~provids~~ provides us with a statistically steady result, and a number of parcels that could still be handled in a finite amount of time in the post processing.

The effect of 1D and 3D thermal radiation on the growth of cloud droplets depends (among other factors) on the length of time that a droplet is exposed to thermal cooling (in other words, that a droplet is located close to cloud edges/cloud top) and the strength of the cooling. Harrington et al. (2000) found that droplets have to spend about 10 min in a cooling area to experience a noticeable effect in the droplet size distribution. We therefore first investigated different properties of our trajectories:

- In-cloud residence time
- Time spent in the vicinity of cloud edges/tops

For the cloud residence time, we used a threshold of 0.01 gkg^{-1} to separate between cloudy and cloud free areas. We then traced among our 340,000 parcel the time periods during which a parcel stays in a cloud. Eventually, a parcel can contact a cloud more than once. In that case, the hits were counted as multiple events. Figure ~~**??**~~ 2 shows a histogram of the time that our parcels spend in clouds. Most of the parcels stay less than 15 min in a cloud, but we also find some rather long periods of

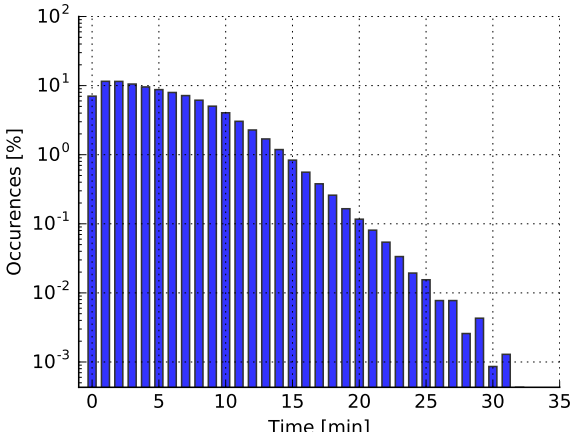

Figure 2. Histogram of the time that parcels spend in a cloud. For the sampling of the data, a threshold of 0.01 gkg^{-1} of the ~~q_c~~ q_c was used to separate cloudy from non-cloudy regions.

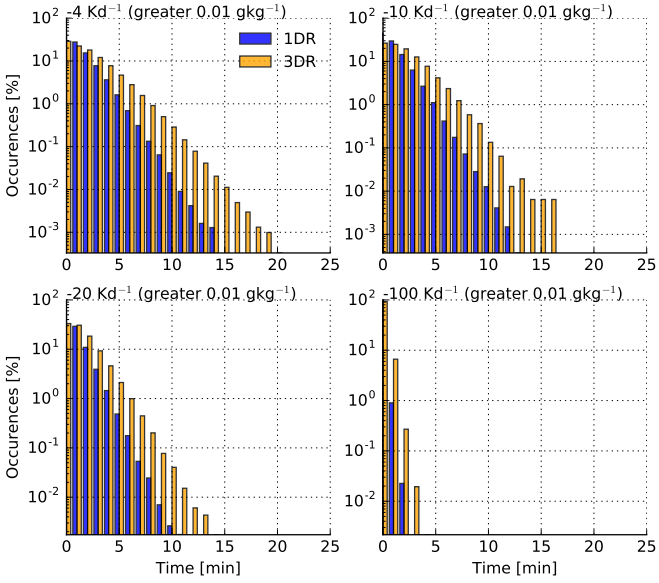

Figure 3. Histogram of the time that parcels spend at cloud top or cloud side. For the sampling of the data, a threshold of 0.01 gkg^{-1} of the ~~q_c~~ q_c was used to separate cloudy from non-cloudy regions. To separate cloud edge regions from the cloud interior, 4 different thresholds of the cooling rates were used (4 Kd^{-1}, 10 Kd^{-1}, 20 Kd^{-1}, 100 Kd^{-1}).

more than 25 min. This is in agreement with former results (e.g. ~~(Jiang et al., 2010)~~Jiang et al. (2010)) for BOMEX.

The time at cloud side was estimate by a) setting the same threshold for the ~~q_c~~ q_c (0.01 gkg^{-1}) and additionally setting four

different thresholds in terms of heating rates (-4 Kd^{-1}, -10 Kd^{-1}, -20 Kd^{-1}, -100 Kd^{-1}) for 1D and 3D thermal radiation. Again, multiple hits were possible for each parcel trajectory. The histograms are shown in Fig. ??3. 1D (blue) and 3D (orange) thermal radiative transfer simulations show that most of the parcels spend less than 5 min in a certain cooling volume encompassing a cooling threshold. For the 100 Kd^{-1} threshold, no parcel ~~exceedd~~ exceeds 3 minutes. However, there are some parcels which spend 10 min or longer, especially when 3D radiative effects are considered in volumes experiencing cooling of 10-20 Kd^{-1}. This is simply due to the fact that a larger volume of each cloud experienced cooling rates in 3D radiative transfer. The possibility that thermal radiation can affect cloud droplet growth is therefore given. In the following, we will take a closer look at individual parcel trajectories and the overall statistics of the 340,000 parcel trajectory ensemble.

4.2 Parcel Model - Cloud Droplet Growth including Thermal Radiative Effects

4.2.1 Individual Parcels

We now focus on individual parcels. An example of a parcel trajectory is given in Fig. ~~??. The q_c~~ 4. The q_c is shown in color (Fig. ~~??~~ 4 a). This illustration of the trajectory includes a temporal dimension. Each data point is recorded at a different time step. The parcel rises in the beginning, enters an area of high ~~q_c~~ q_c (red, arrow i)), followed by a decrease in ~~q_c~~ q_c (blue area, arrow ii)), but never drops to zero, before entering again an area of high ~~q_c~~ q_c (red, arrow iii)). Finally, ~~q_c~~ q_c decreases again and the parcel leaves the cloud.

The other three figures of Fig. ~~??~~ 4 combine time snapshots of the cloud field and the temporal development of the parcel trajectory. The cloud field is shown at the time marked by the red dot on the trajectory. The surface shows the liquid water path, ~~lwp~~lwp, of the selected cloud field at that specific time. The red dot on the surface is the vertical projection of the location of the parcel at the time. Figure ~~??~~ 4 b) shows the updraft area where the parcel first enters an area of high ~~q_c~~q_c. The parcel (at that time) is located in an upper part of the cloud where it experiences cooling. In the following, the cloud grows and at time c) a significantly larger cloud with more ~~q_c~~ q_c is encountered. The parcel is now located at the outer edge of the cloud (especially visible at the ~~lwp~~ lwp field, red dot). ~~q_c~~ q_c has dropped below 0.01 gkg^{-1}, but does not decrease to zero in the following, meaning the parcel never leaves the cloud. The cloud grows further in the following (Fig. ~~??~~ 4 d)) and the parcel is located again in an area of high ~~q_c~~q_c. We will see later that this 'recirculation' of parcels occurs occasionally and can cause a broadening in the droplet size spectrum. It is likely that radiative effects become more important in this case, because parcels pass cloud edges where thermal cooling per droplet is strong.

Parcel Trajectory 1

We now take a more detailed look at the ~~parcel trajectory~~ same parcel trajectory as shown in (Fig. ~~5). This selected parcel~~4). Figure 5 shows this selected parcel, which is characterized by moderate vertical velocities (peaking at about 6 ms^{-1} in the beginning, but not exceeding 2 ms^{-1} later on). The parcel stays in the cloud for about 20 minutes and twice experiences radiative cooling (for about 8 minutes and 2 minutes). We chose four different time steps for further investigation (red dotted lines at 14, 16, 21 and 25 minutes). The first time step was chosen shortly after the parcel passes the first volume of strong cooling and is

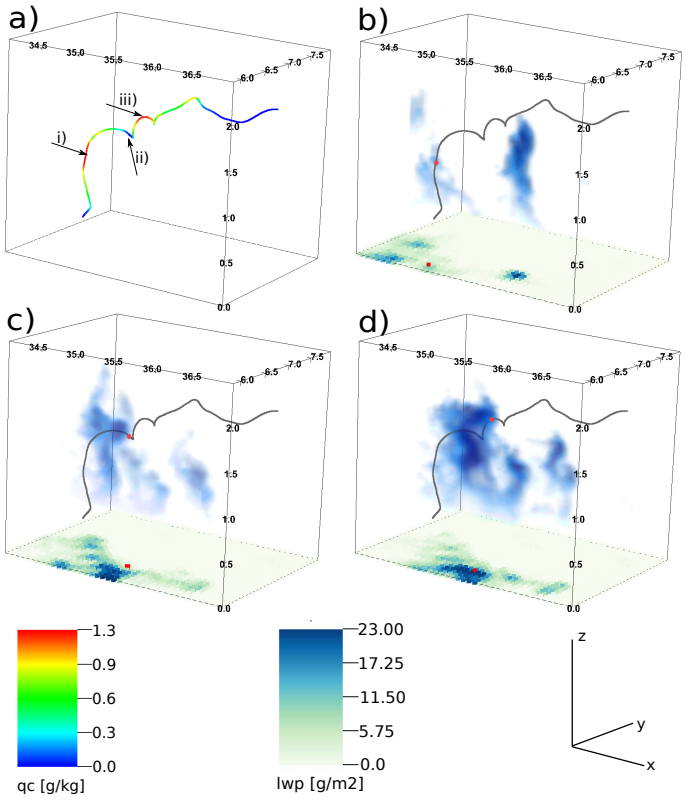

Figure 4. 3D Visualization of ~~q_c~~ q_c, the parcel position and ~~lwp~~ lwp of the selected scene. The first figure (upper left) shows the parcel trajectory. The ~~q_c~~ q_c at each time step of the selected parcel is colored. Three time intervals were selected for the following figures: time intervals where ~~there~~ the parcel stays in high ~~q_c~~ q_c areas (i,iii) and one, where the ~~q_c~~ q_c drops ~~significantly~~ substantially but does not reduce to zero (i). The following 3 figures show the parcel trajectory (gray, again time dependent). For the time interval in focus, the ~~q_c~~ q_c is again colored. The displayed clouds are chosen at the center time of the interval, as is the ~~lwp~~lwp. The red marker displayed in the ~~lwp~~ lwp field shows the projected location of the center time step.

recirculating. Here, we defined 'recirculation' loosely as an event where the ~~q_c~~ q_c along a parcel trajectory becomes very low (in this case 0.007 gkg^{-1}). The second time step was chosen after ~~q_c~~ q_c has risen again, the third time step shortly before the second cooling phase, and the fourth when the parcel leaves the cloud.

The drop distribution at these four time steps is shown in Fig. 6. The upper figures show the drop spectra (dm/dr) themselves, the lower figures the ratio of the spectra of the 1DR/3DR simulations and the NR simulation of the parcel.

In the beginning, hardly any differences can be seen in the drop spectra between the NR, 1DR and 3DR simulations. The spectrum broadens over time. Looking at the ratio of dm/dr of the 1DR/3DR and the NR simulation reveals a decrease in mass in the small bins and an increase in the larger bins for the radiation simulations. This changes later in the simulation when the simulations with thermal radiation increase mass over the whole drop spectrum. dm/dr for the 1DR and 3DR simulations exceeds the NR simulations up to 1.5 times for ~~r~~ r > 10 μm. The size spectrum broadens and a drizzle mode develops. The

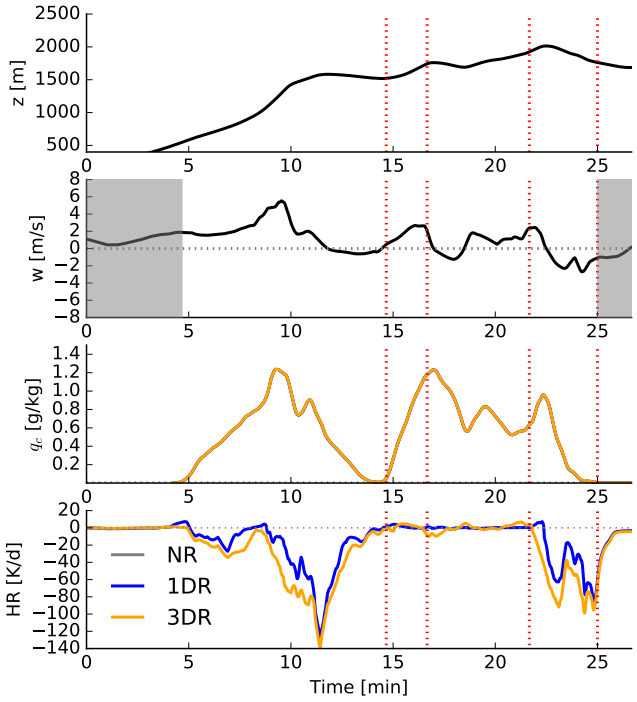

Figure 5. ~~Timeseries~~ Time series of different properties of the first selected parcel. Shown are: height, vertical velocity, ~~q_c~~ q_c, heating/cooling rate, predominant radius and the heating/cooling rate per droplet. Gray areas show time intervals where the ~~q_c~~ q_c is below 0.01 gkg^{-1}. The red dotted lines show selected time steps used in the following analysis.

peak of the spectra remains at about 15 μm. The ratio for 3DR simulations always exceed that for 1DR simulations. A factor of more than 2 is reached for dm/dr of the 3D radiation simulation compared to the NR simulation. The droplet concentration in the 20 μm bin (not shown) increases by up to 15% for the 3DR case along this trajectory.

The possible increase in droplet growth by thermal radiation does not only depend on the time that a droplet is exposed to cooling, but also on the magnitude of the cooling and the size of the droplet. The larger the droplet, the more effectively radiation can act on it as the droplet absorbs and emits radiation more effectively. Radiative effects become stronger from a radius of about 10 μm on. Additionally, the radiative impact competes with the dynamical effects, which depend on the vertical velocity (see Eq. (7)). It therefore follows that the larger the droplet and the weaker the updraft, the more radiation can affect droplet growth. Figure 7 shows the temporal development of the individual droplet heating/cooling rate for ~~four~~ three different sizes (left column). This heating/cooling rate is the fraction of the spectrally- and bin-integrated cooling rate per bin (Eq. (4)), integrated over all wavelength. The center radius of the corresponding bin is given in each figure. Gray shaded areas and the red lines are identical to those shown in Fig. 5 for comparison. Note the change in the y-axis for these figures. We find that the

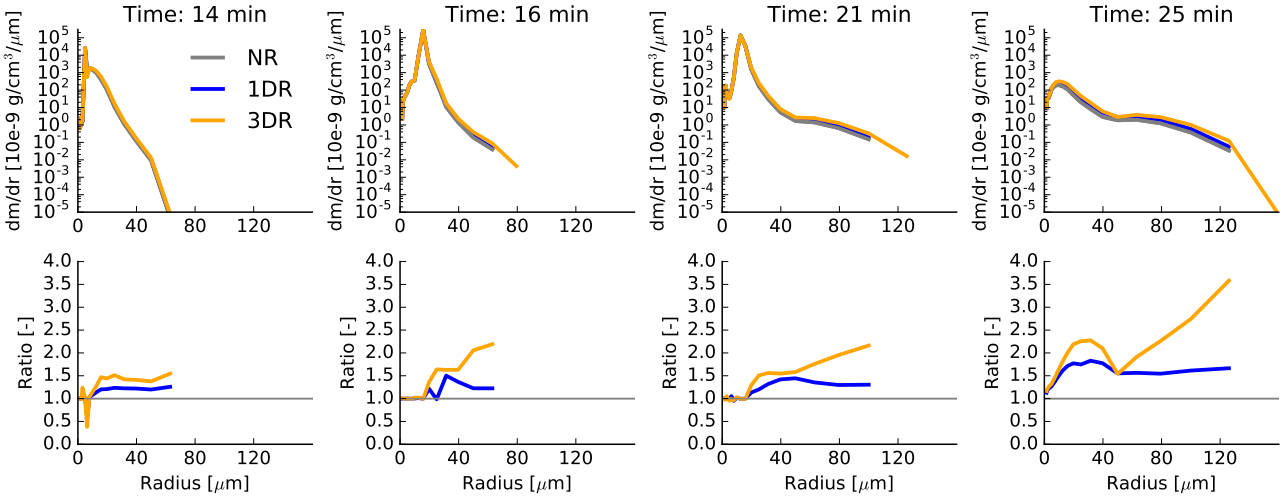

Figure 6. Drop size distribution dm/dr plot for the four selected time steps displayed by the red dotted line in Fig.5. The upper row shows dm/dr. The lower row shows the ratio between the NR case and the 1DR/3DR case. Gray areas in the lower row display size bins where mass occurs in the 1DR/3DR case, but not the 1DR case and wherefore no ratio could be calculated.

cooling per droplet increases with increasing radius and that 3D cooling is stronger than 1D cooling.

The right column shows the forcing τ (Eq. (7)), which is the total effect on the mass in each bin. The gray line shows the dynamical forcing (τ_d), which, if compared to Fig. 5 follows the vertical velocity trend. The radiative forcing (τ_r) is shown in yellow (3D) and blue (1D) for the same four size bins. Note that a cooling per droplet (left side) causes a positive contribution to the droplet growth and therefore a positive forcing (right side). The radiative forcing is smaller than the dynamical one but has the same order of magnitude. An additional boost is given to the droplet growth shortly before 15 min before the dynamical forcing rises again. This small radiative perturbation is sufficient to cause the increase in dm/dr seen in the second column of Fig. 6. The radiative forcing becomes strongest towards the end of the parcel trajectory, counteracting the negative dynamical forcing, especially for the larger size bins.

Parcel Trajectory 2

This second parcel experiences stronger dynamical forcing. Vertical velocity rises and falls throughout the parcel's lifetime and peaks at more than +/- 6 ms^{-1}. The parcel recirculates twice. During these two periods the parcel experiences radiative cooling, which causes a broadening of the droplet size spectrum (Fig. 8 and Fig. 9). Due to the strong dynamical forcing, the parcel shows broader spectra than the first trajectory. As before, a ~~significant~~ substantial increase in condensed water is found for the 1DR and 3DR simulations, peaking for the 3D thermal radiation simulation.

These examples illustrate the ~~the~~ variety of ways in which radiative effects can act on a cloud droplet. The time that a parcel spends in a certain cooling area, the magnitude of the cooling, the size of the droplets at the time of cooling and the dynamical

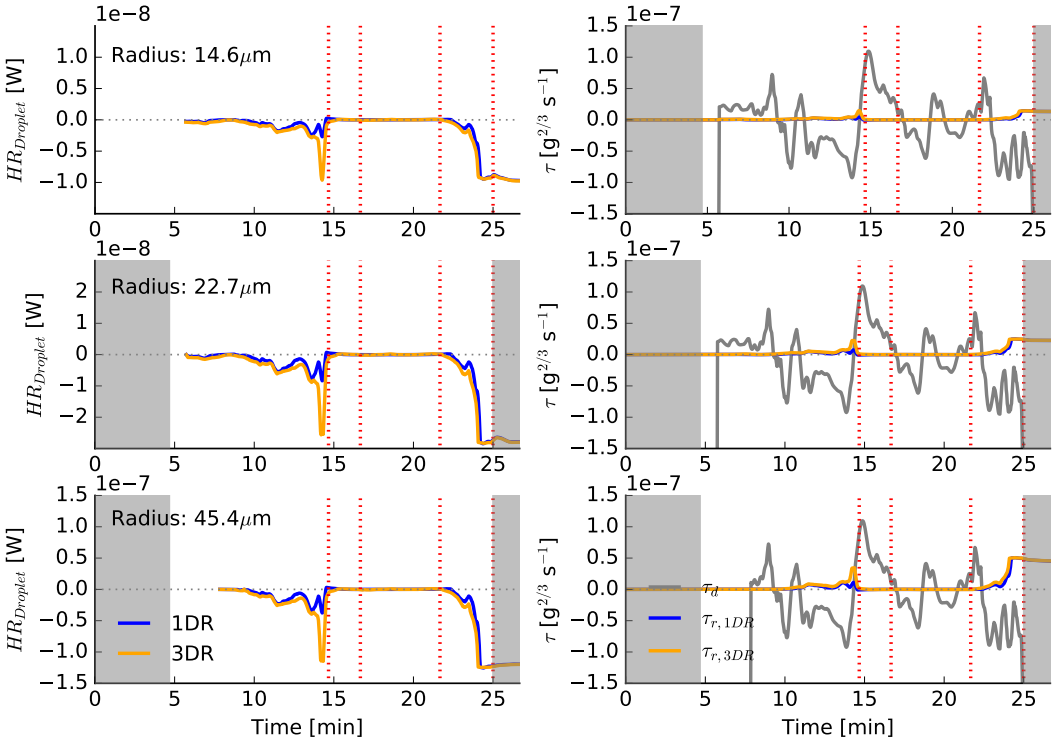

Figure 7. Wavelength integrated, bin-resolved heating/cooling rates and forcing τ_d and τ_r

forcing contribute to droplet growth with different magnitudes. The ideal situation for the radiative effects to enhance droplet growth would be droplets of size of about 10 μm or more, a cooling period of more than 5 minutes in a cooling of 20 Kd^{-1} or more, and vertical velocities close to zero. Because these effects usually do not occur together, the overall effect on the droplet growth from these factors is small.

A strong effect is found when parcels recirculate. Whenever a parcel reaches cloud edge, the number of droplets is small. Yet, these droplets are exposed to cloud top/ cloud edge cooling which, due to the limited number of droplets is close to the maximum cooling that a droplet can experience (2 in Fig. ??10). Additionally, these parcels already include larger droplets, where radiative effects are stronger. The droplets experience additional growth by radiative cooling during the recirculation time and return into the cloud with a slightly broadened size distribution (3 in Fig. ??10). The droplet size distribution subsequently continues to broaden (4 in Fig. ??10).

Summarizing, these analyses of individual parcel trajectories have shown that radiatively enhanced droplet growth can occur in 'lucky situations' or when recirculation occurs. The increased droplet growth for recirculating parcels agrees well with former results of enhanced droplet growth in areas of net radiative loss (see e.g. Caughey and Kitchen (1984)). The radiative cooling

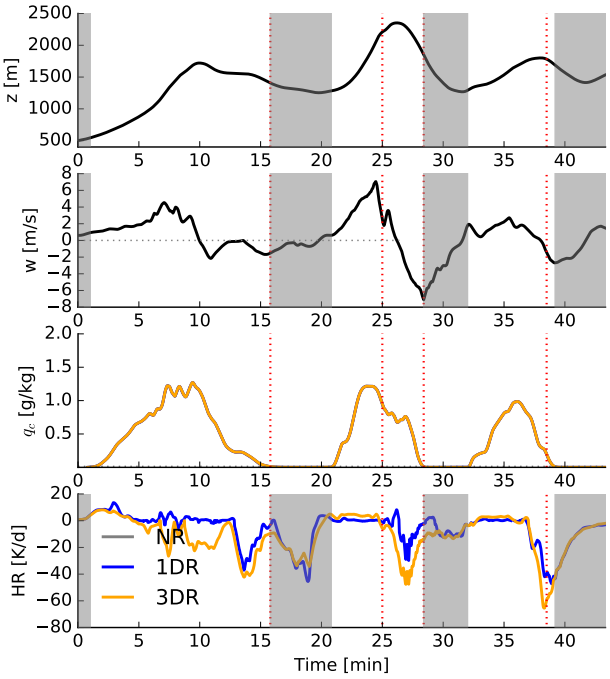

Figure 8. Similar to Fig. 5, but for the second selected parcel.

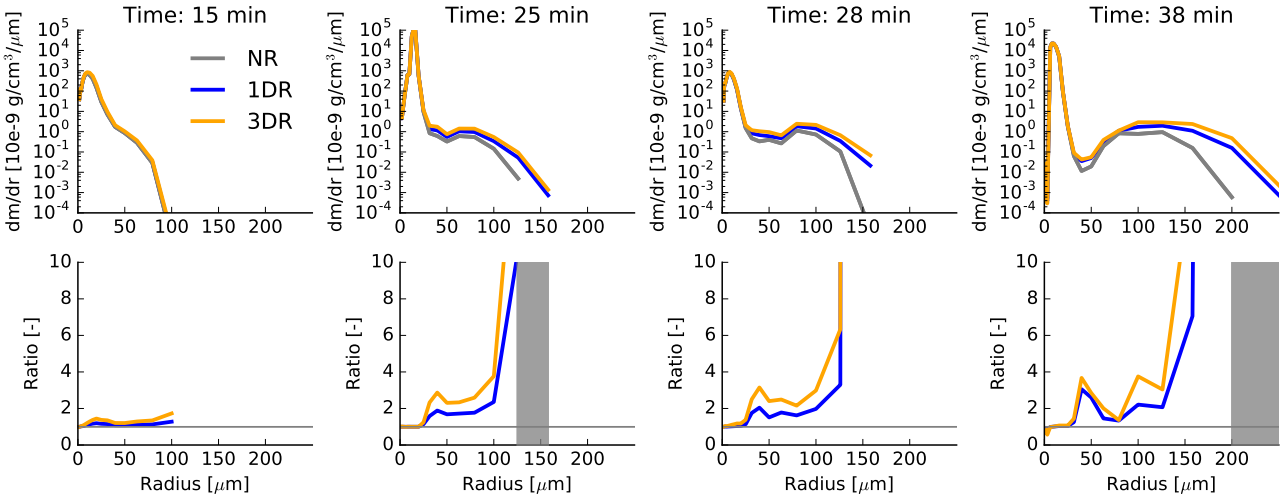

Figure 9. Similar to Fig. 6, but for the second selected parcel.

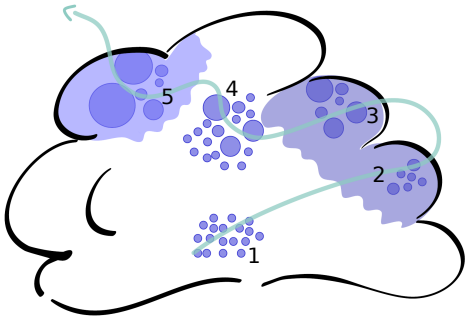

Figure 10. Schematic figure of the droplet growth for a recirculating parcel.

does not seem to cause droplet growth in individual parcels beyond the NR case (as also found by Harrington et al. (2000)), but thermal radiative effects enhance the mass per bin and occasionally allow droplets to grow into larger bins. In the following, we will take a more general look at the effects in our parcel trajectory ensemble.

4.2.2 Parcel Model - Ensemble Results

As a next step, we evaluated our 340,000 parcel trajectory ensemble to see if we find changes in droplet size and rain rate. Figure ~~??~~ 11 shows a histogram of maximum mean radius along a parcel trajectory versus the integrated ~~q_c~~ q_c along the parcels. The first figure shows the number of occurrences for the NR case. Integrated ~~q_c~~ q_c mostly occurs in a range of 0 - 10 g kg^{-1} min with maximum mean radii up to 20 μm. Larger droplets and integrated ~~q_c~~ q_c amounts exist, but are comparatively small in number. When comparing the number of occurrences of the 1DR case to the NR case, we find an increase in the number of larger droplets for small ~~q_c~~ q_c amounts and for those between 5 to 10 g kg^{-1} min and a decrease in the directly smaller bin. Radiation thus enhances the growth of droplets for a specific ~~q_c~~ q_c for very small droplets and for droplets in the 10 - 25/30 μm range. There is also a tendency for the larger drops to grow to larger sizes in the 1DR case. For 3D thermal radiation we see a similar picture. The number of droplets growing to larger sizes is even higher than in the 1DR case. Comparing the results of the 3D thermal radiative transfer simulation to the 1DR simulation shows the additional increase in the 3DR case. We confirm here that due to thermal radiation droplets in the critical range tend to grow to larger sizes.

Next, we calculate the ~~rain rate~~ vertically integrated rain rate (by integrating the size bins from 20 μm on) along our trajectories for the entire ensemble. In the first hour, the absolute differences in the rain rate between the three setups is small. Absolute differences get larger over time and are clearly visible during the last 40 min of the analyzed time period (Fig. ~~??~~12). Looking at the relative differences between either the 1DR simulation and the NR case, or 3D thermal radiation simulation and the NR case, we find differences of 10% for the 1DR case in the first hour, and 20% for the 3D thermal radiation case. Relative differences increase ~~commensuratly~~ commensurately with the absolute differences towards the end of the 2 hour simulation and reach as high as 40% for the 3D thermal radiation case.

We then separated the rain rates according to different factors that could affect droplet growth on our trajectories. Following

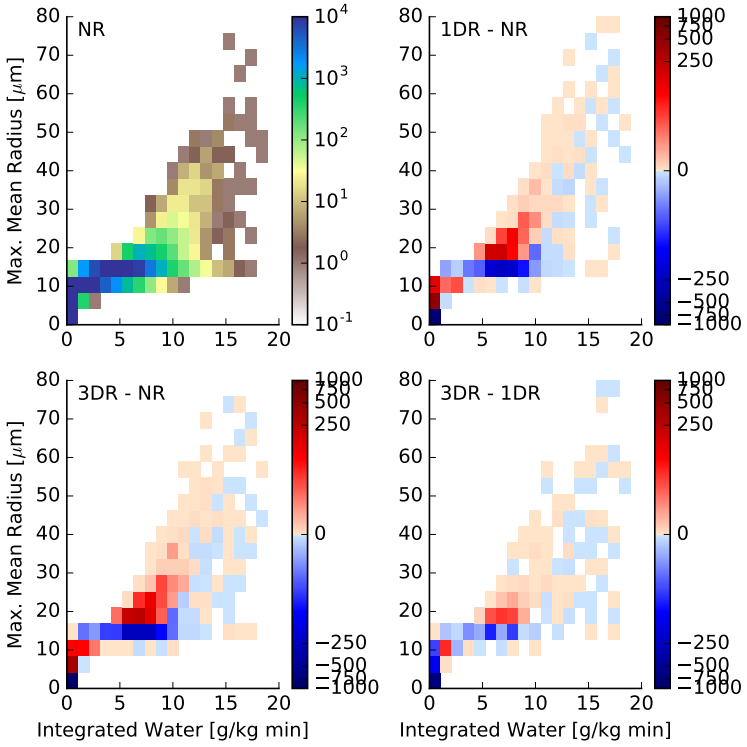

Figure 11. Joint histogram of integrated water and maximum mean radius. The first figure shows all data from the NR simulation. The other figures show the difference of the number of occurrence of 1DR vs NR, 3DR vs. NR and 3DR vs. 1DR.

on the results of our investigation of the individual trajectories, we calculated rain rates for parcels with certain thresholds of updraft speeds, cumulative cooling, or time spent at cloud side. About 50% of the rain rate arises from parcels that are in an updraft region of 3 ms^{-1} or more (regions typically associated with higher q_c), but differences between the NR and 1DR/3DR cases are small. The largest radiative effect emerges from parcels that recirculate (see Fig. ??14). We define 'recirculation' by setting a threshold in terms of ~~q_c~~ q_c of 0.01 gkg^{-1}.

~~Up to 60~~The time periods for recirculation events are shown in Fig. 13. Most of the parcel spend a few minutes outside a cloud. More than 90% of the recirulation events are shorter than 5 minutes. Up to 58% of the accumulated rain rate of the 3DR simulation arises from recirculating parcels, while in the case of NR, about 45% of the accumulated rain rate ~~comes~~ arises from recirculating parcels. The largest increase is found within the last 20 minutes of the investigated timeframe. Differences of 5-10% are found in the first 20 to 50 minutes, while in between, there is no difference between the three simulation types. Setting an upper limit in time (e.g. 5 min, which includes more than 90% of our recirculating parcels), the changes in our results are very small. The maximum contribution of the rain rate reduces to 56%. For a time threshold of 2 min, the maximum reduces to 45%. In this context it should be noted that only 6-7% of our 340,000 parcel trajectories are classified as recirculating according to our definition. Remarkably, these 6-7% can contribute up to 60% of the accumulated rain rate. The accumulated

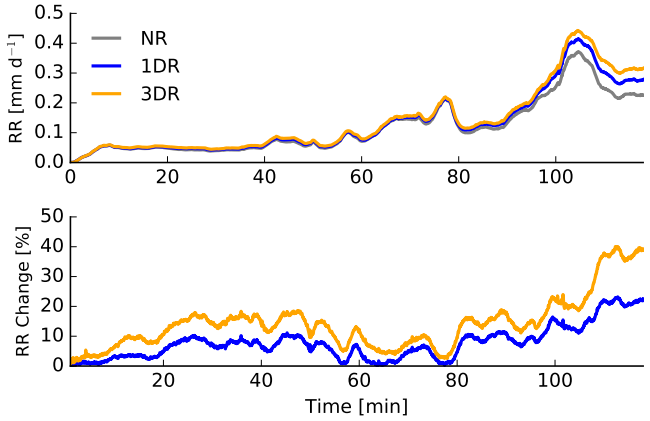

Figure 12. ~~Rain~~ Vertically integrated rain rate calculated from the ensemble parcel simulation (by integrating the size bins from 20 μm on). The top panel shows the absolute rain rate for the NR, the 1DR and the 3DR cases. The bottom panel shows the relative differences of 1DR simulation and the NR case, and 3DR simulation and the NR cases.

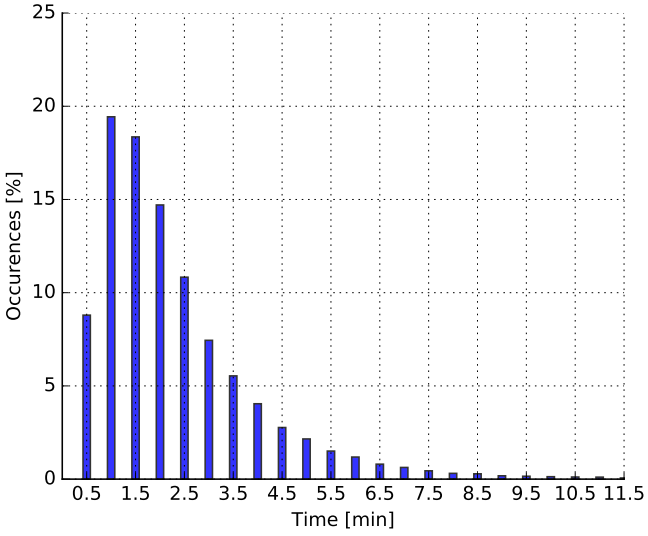

Figure 13. Histogram of the time period of recirculation events. Recirculation events are defined by threshold in terms of q_c of 0.01 gkg^{-1}.

rain rate due to recirculation (when normalized to each of the corresponding simulations and therefore without considering radiative effects) is about 30% in our study. Naumann and Seifert (2016) found a similar magnitude in their study. About 50% of the rain rate emerged from recirculating parcels. These zones might be considered the birth place of precipitation embryos, which, subsequently become important for accelerating collision and coalescence.

5

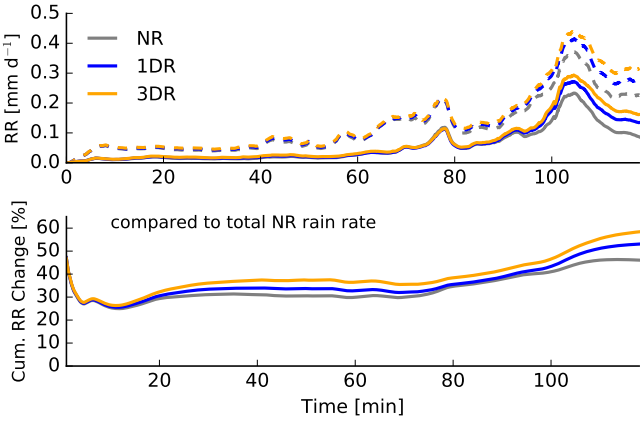

Figure 14. ~~Rain~~ Vertically integrated rain rate from recirculating parcels, threshold 0.01 gkg^{-1}. The dashed lines show the total rain rate, the solid line the rain rate from recirculating parcels as well as the relative difference between the rain rates from recirculating parcels compared to the total NR rain rate.

4.3 Coupled LES Simulation - Cloud Droplet Growth under the Impact of Thermal Radiative Effects

Next, we investigate the effect of 1D and 3D thermal radiation in a fully coupled system. To this end, we ran a set of BOMEX simulations as described in Section 3. Here we a) look at the effects of thermal radiation on microphysics in a coupled system and b) compare it to the effect on dynamics.

4.3.1 The Effect of Thermal Radiative Transfer on Microphysics

We start with variables concerning rain, and first focus on the microphysical effect. Figure ~~??~~ 15 shows rain water path, surface precipitation fraction, domain-averaged surface precipitation rate and the cumulative surface precipitation rate of 4 of the 5 simulations. We take the simulation with 1D radiation on dynamics ($1DD$) as our reference case. ~~As it is the least noisy field, we focus~~ We focus first on the discussion of the rain water path~~first~~. We find a small increase in rain water path an hour after restart in the case of 3D radiation acting on microphysics and dynamics ($3DD\_3DM$)~~. Differences become larger but also noisier two hours after restart. The other 3 simulations do not show a significant difference~~, however differences amongst the four simulations never become significant. Surface precipitation fraction (over the total domain) shows an increase for all simulations where radiation is coupled to the diffusional droplet growth. The strongest increase is found for the $3DD\_3DM$ case. This suggests that more clouds produce rain when radiation is coupled to the droplet growth, but the total amount of rain water produced does not change substantially.

The surface precipitation rate shows no observed changes, but in accumulation, the simulations with the radiative-microphysical coupling produce more rain (10% for $3DD\_3DM$). There is a subtle increase in ~~rain~~ the accumulated rain rate and rain

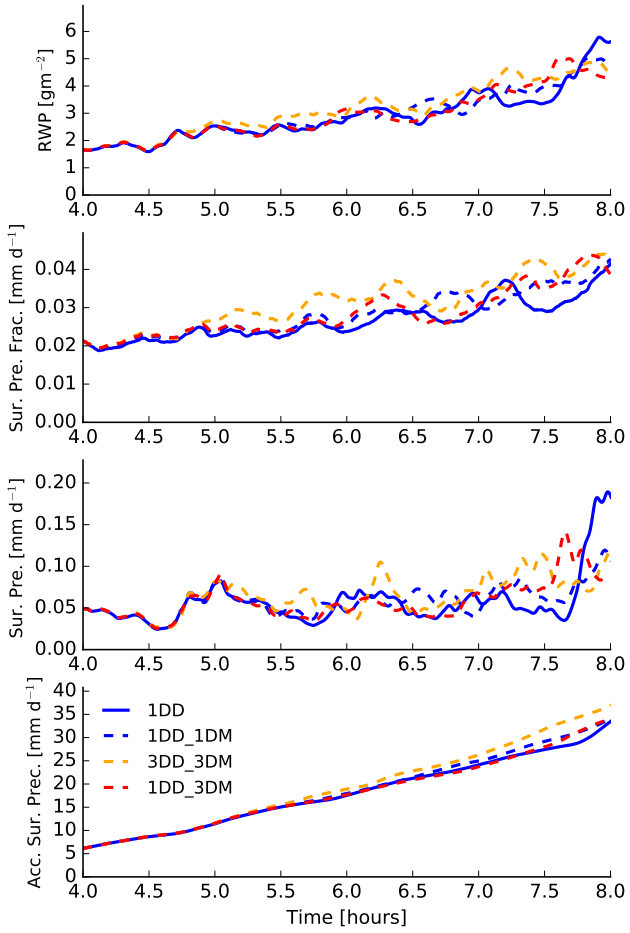

Figure 15. Temporal development of rain water path (top), surface precipitation fraction (second from top), domain averaged surface precipitation rate (second from bottom) and the accumulated domain averaged surface precipitation rate (bottom). The time series is shown from the restart time of 4 hours onward. We compare four of our five simulations here where thermal radiation was coupled to the diffusional droplet growth.

water path when thermal radiation is coupled to the diffusional droplet growth. However, when comparing $1DD\_3DM$ to $1DD\_1DM$, no difference can be found. Hence, the small increase in rain in the case of $3DD\_3DM$ must arise from the effects of 3D thermal radiation on dynamics, not on microphysics. We will investigate the 3D effect further in the following.

~~Surface precipitation fraction shows an increase for all simulations where radiation is coupled to the diffusional droplet growth.~~

~~The strongest increase is again found for the $3DD\_3DM$ case. This suggests that more clouds produce rain when radiation is coupled to the droplet growth, but the total amount of rain water produced does not change significantly.~~

4.3.2 3D Thermal Radiative Effects

Figure ~~??~~ 16 shows the same variables as Fig. ~~??~~ 15 but now comparing the results of the $3DD\_3DM$ and $3DD$. In the beginning, rain water path and rain rate show no ~~significant~~ considerable difference. After 7 hours of the simulation, rain water increases for $3DD$. Before 7 hours, as also discussed in 4.3.1, the fraction of surface rain rate is slightly enhanced in $3DD\_3DM$ compared to $3DD$, which again suggests that the coupling to microphysics does not produce more rain but that more clouds produce small amounts of rain, while in the $3DD$ case changes in the dynamics cause somewhat stronger rain in fewer clouds. The lower figure shows again the accumulated surface rain rate over time. The $3DD$ simulation produces more rain. This was counterintuitive at first, because it was expected that thermal radiative effects enhance droplet growth.

We pose the following hypothesis to explain this behavior:

Enhanced droplet growth, due to 3D thermal radiation at the cloud edges decreases the evaporation at the cloud edges causing weaker evaporative cooling, and weaker downward motion, representing an evaporation-circulation feedback

This hypothesis constitutes a negative feedback to changes in the cloud circulation found by Klinger et al. (2017), and will be explained in the following. It is analogous to the previously documented evaporation-circulation feedback due to changing aerosol concentrations in cumulus clouds (Xue and Feingold, 2006) and earlier studies that identified the relationship between the horizontal buoyancy gradient and the vortical circulation around a cloud; stronger ~~stronger~~ cloud edge evaporation generates stronger horizontal buoyancy gradients, increased TKE and enhanced mixing and entrainment (Zhao and Austin, 2005).

Klinger et al. (2017) found an enhanced cloud circulation due to thermal radiative effects. It was shown that cloud top cooling caused stronger updraft velocities in the clouds, and due to the side cooling stronger subsiding shells at the cloud edge. Due to the stronger updrafts, clouds were deeper, more turbulent, and contained more ~~q_c~~q_c. The results from Klinger et al. (2017) and the above posed hypothesis, can, if correct, explain the differences in surface rain fraction and rain rate between the two simulations. We will therefore investigate the profiles of cloud water mixing ratio, precipitation flux, evaporation rate and buoyancy production of TKE (Fig. ~~??~~17), averaged over half an hour marked by the gray shading in Fig. ~~??~~16. This time period is chosen as it is the period shortly before and at the beginning of the increase in rain production. All four variables show higher values for $3DD$ compared to $3DD\_3DM$. Finally, we look at the temporally averaged profiles of updraft and downdraft vertical velocities in saturated areas. Here we also find stronger downdraft and stronger updrafts in the $3DD$ case. These analyses lend credence to our hypothesis, and Klinger et al. (2017) (Fig. ~~??~~18).

4.3.3 1D vs 3D Thermal Radiative Effects

Finally, we compare the results of $1DD$ and $3DD$ to examine the effect of 3D thermal radiation on dynamics. We set the focus again on rain production as this was not included in Klinger et al. (2017). As expected, 3D radiation causes an increase in all

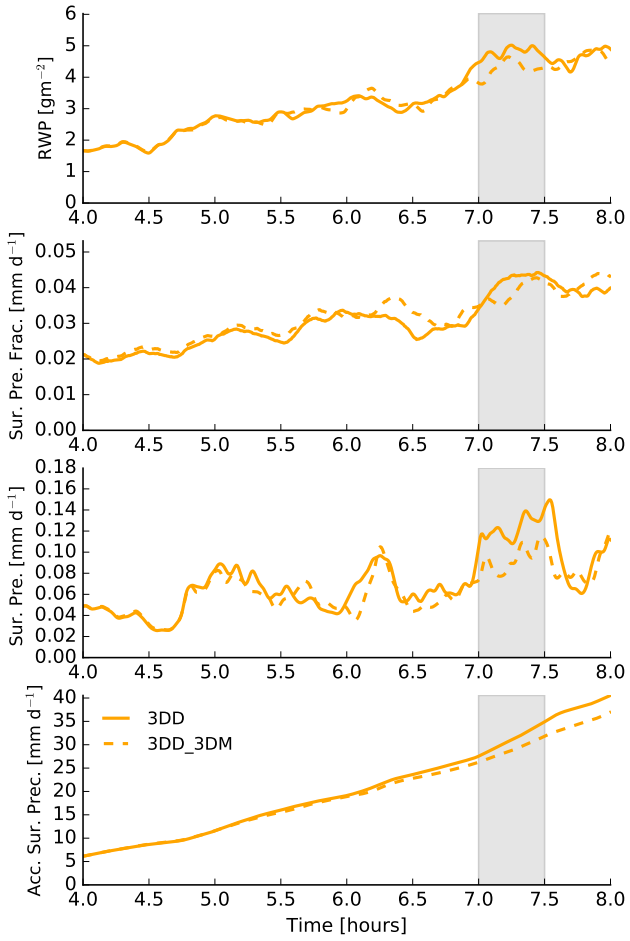

Figure 16. Similar to Figure ??15 but for $3DD$ and $3DD\_3DM$. The gray shaded area show the time period between 6.7 and 7.3 hours which is investigated in the further analysis.

the rain-related variables (shown in Fig. ??19). To prove that a change in the cloud circulation is also causing the increase in rain, we look at the profiles of the updraft and downdraft vertical velocity in saturated areas, averaged over two time periods marked in gray in Fig. ??19. The time periods were again chosen because they include the beginning of rain enhancement by 3D thermal radiation compared to 1D thermal radiation. For both time periods, Fig. ??20 shows enhanced downdrafts and updrafts for the $3DD$ simulation compared to $1DD$.

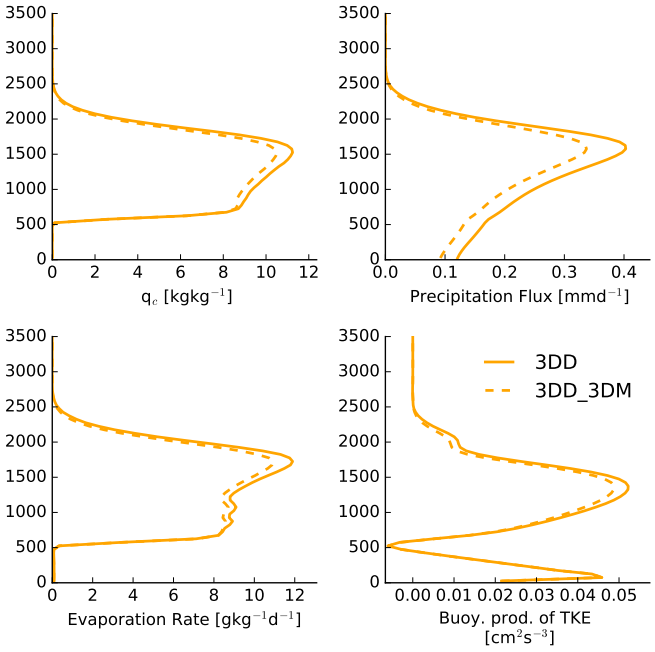

Figure 17. Time averaged profiles of cloud water mixing ratio, precipitation flux, evaporation rate and buoyancy production of the TKE averaged from 6.7 to 7.3 hours.

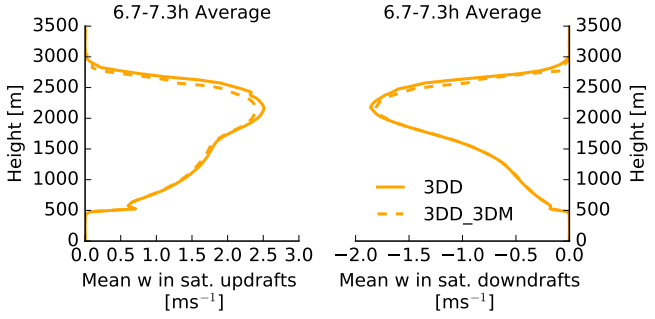

Figure 18. Time averaged profiles of updraft and downdraft vertical velocity in saturated areas averaged from 6.7 to 7.3 hours.

4.3.4 Summary

~~To summarize the results from the coupled large eddy simulations we find~~The coupling of thermal radiative effects to microphysics can lead to the formation of larger cloud droplets and drizzle droplets. For 3D thermal radiative effects, additioinal cooling occurs at cloud edges which can strengthen the effect. The coupled LES simulations showed that:

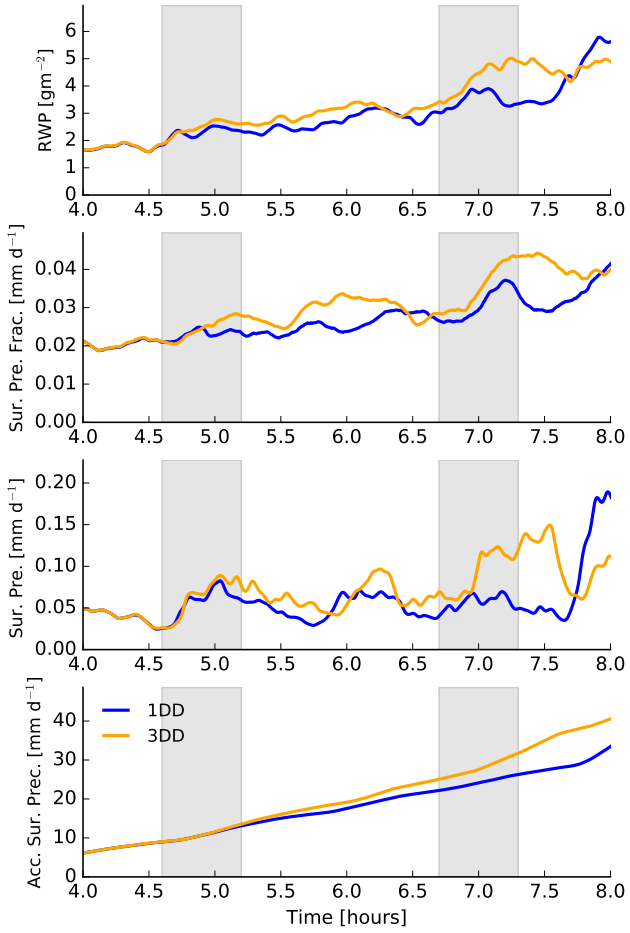

Figure 19. Similar to Fig. ~~??~~ 15 but for $1DD$ and $3DD$. The gray shaded area show the time period between 4.6 and 5.3 hours as well as 6.7 and 7.3 hours which are investigated in the further analysis.

– When thermal radiation is coupled to microphysics, there is a small increase in rain production for 1D radiative effects ($1DD\_1DM$). This could be due to recirculation of droplets as was shown in the parcel model study. However, the change of rain in the coupled simulations is very small. When coupling radiation to droplet growth it matters little whether 3D or 1D thermal radiation is applied. The increase in the surface precipitation fraction suggests that rain is produced in more clouds distributed over the domain.

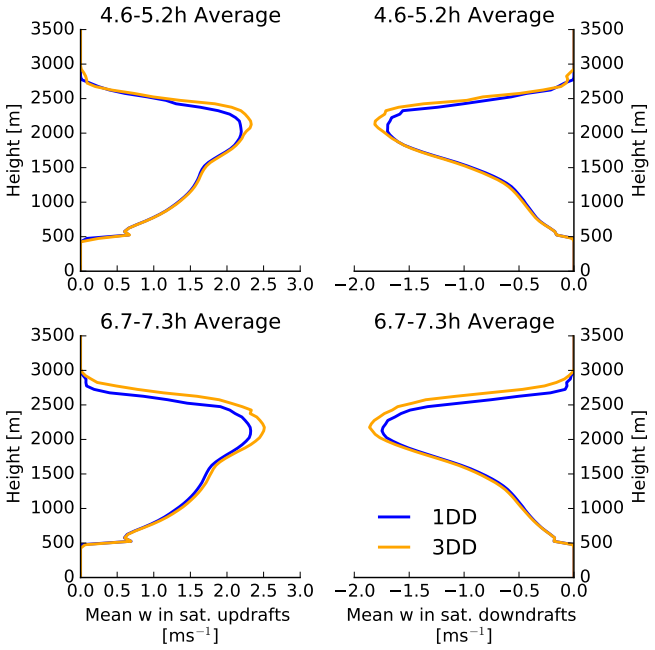

Figure 20. Similar to Fig. ~~??~~ 18 but for $1DD$ and $3DD$ and for the time period between 4.6 and 5.3 hours as well as 6.7 and 7.3 hours.

- When 3D thermal radiative effects are considered we find (counterintuitively) overall more rain in the simulation with dynamics only.
- The fact that more rain is produced by the simulation coupled to dynamics only is hypothesized to be due to an evaporation-circulation feedback caused by the larger droplets in the $3DD\_3DM$ simulation.
- When comparing the 1D and 3D thermal radiative effects on dynamics we find an increase in the rain production for 3D thermal radiation.
- The dynamical effect caused by 1D and 3D thermal radiation is a change in the cloud circulation as already found by Klinger et al. (2017) where thermal radiation increases upward and downward vertical velocities in and in the near cloud environment, which causes deepening and more rain.

Finally, we note that the overall differences concerning precipitation are small and might not be detectable relative to differences associated with perturbations to thermodynamical inputs in an ensemble of simulations (see eg. Lonitz et al. (2015)).

5 Conclusions

In this study we investigated the effect of thermal radiation on cloud droplet growth and rain formation in shallow cumulus clouds. We used a two stage approach which allowed us to separate microphysical from dynamical effects.

First an offline parcel model was used to investigate the effect of 1D and 3D thermal radiation on cloud droplet growth. It was found that thermal radiation in general can enhance droplet growth and rain formation. 3D thermal radiation enhances droplet growth and rain formation more than 1D thermal radiation. It was shown that thermal radiation enhances droplet growth especially in the 10-30 μm region. Thermal radiation can affect cloud droplet growth when one or more of the following conditions are fulfilled:

Droplets have already grown to a size of about 10 μm or more when being exposed to thermal cooling. A cooling period of more than 5 minutes at a cooling rate of 20 Kd^{-1} or more, and vertical velocities close to zero are favorable for radiative effects. If one or more of these factors occur, radiative cooling can enhance droplet growth. The main effect was found from recirculating parcels which fulfill parts of the abovementioned criteria. Recirculating parcels include droplets that have already grown to a certain size when passing a cloud edge area. At the cloud edge area cloud droplets are exposed to large cooling (close to black body emission) and this small number of droplets grows by thermal cooling which counteracts evaporation. When reentering a cloud, droplet growth continues, generating a broader spectrum, which can enhance rain formation. Only 6-7$\%$ of our simulated parcels are classified as recirculating, yet they can contribute up to 45-60$\%$ of the rain rate.

Second, in a more realistic framework we investigated large eddy simulations where thermal radiative effects were applied to droplet growth and dynamics. It was shown that the effect on droplet growth is small. However more clouds produce small amounts of rain when radiative effects are applied to the diffusional droplet growth; thus rain covers a larger area of the simulation domain. 3D thermal radiative effects exceed 1D thermal radiative effects. The largest amount of rain is produced when 3D thermal radiation is applied to dynamics only. This was initially considered to be counterintuitive since both microphysical and radiative effects tend to enhance rain. We hypothesize that an evaporation-circulation feedback is responsible for less rain in the simulation where radiation is also applied to droplet growth. 3D thermal cooling rates at the cloud edges enhance droplet growth locally at the cloud edge, thus leading to weaker evaporation rates, which in turn reduces the strength of the subsiding shell and the horizontal buoyancy gradient, all leading to weaker cloud turbulence and lower rain production. In simulations with 3D thermal cooling only applied to the dynamics, the enhanced cloud circulation causes stronger updrafts in the cloud center, a cloud deepening and more condensation/ rain formation.

These results could have implication in terms of cloud field organization. As shown by Klinger et al. (2017) thermal radiation can cause mesoscale organization of shallow cumulus clouds by changing cloud circulation. It was shown that this change in cloud circulation also occurs in the simulation in this study. Furthermore, more rain produced by thermal radiation changes the dynamics of the system as a whole. The larger area of the domain covered by rain when radiative effects are applied to microphysics could also lead to a feedback in terms of dynamics and cloud field organization. Longer simulations are necessary to investigate the organization feedbacks. Finally, a trade-wind cumulus case that tends to deepen and generate more precipitation

and organization would be worth investigating.

~~*Code availability.* Input files and the model code for reproducing the simulations and data of this study are available from the corresponding author upon request.~~

Code availability. Input files and the model code for reproducing the simulations and data of this study are available from the corresponding author upon request.

~~*Competing interests.* The authors declare that they have no conflict of interest.~~

Competing interests. The authors declare that they have no conflict of interest.

Author contributions. CK implemented the 3D radiative transfer scheme into the LES, run the simulations and performed the analysis. TY implemented the bin microphysics scheme into the LES. All authors contributed to developing the basic ideas, discussing the results, and preparing the manuscript.

Acknowledgements. The authors acknowledge Bernhard Mayer and Jerry Harrington for useful discussion and Jan Kazil for help with SAM. We gratefully acknowledge Marat Khairoutdinov (Stony Brook University) for developing and making the System for Atmospheric Modeling (SAM) available. The project was founded by the 'German Research Foundation' (DFG, Research Fellowship KL-3035/1) and the Federal Ministry of Education and Research (BMBF) through the High Definition Clouds and Precipitation for Climate Prediction project (HD(CP)^2) phase 2 (Förderkennzeichen: 01LK1504D). The authors acknowledge the NOAA Research and Development High Performance Computing Program for providing computing and storage resources that have contributed to the research results of this paper.

References

Ackerman, A. S., Hobbs, P. V., and Toon, O. B.: A Model for Particle Microphysics, Turbulent Mixing, and Radiative Transfer in the Stratocumulus-Topped Marine Boundary Layer and Comparisons with Measurements, Journal of the Atmospheric Sciences, 52, 1204–1236, https://doi.org/10.1175/1520-0469(1995)052<1204:AMFPMT>2.0.CO;2, http://dx.doi.org/10.1175/1520-0469(1995)052<1204:AMFPMT>2.0.CO;2, 1995.

Austin, P. H., Siems, S., and Wang, Y.: Constraints on droplet growth in radiatively cooled stratocumulus clouds, Journal of Geophysical Research: Atmospheres, 100, 14 231–14 242, https://doi.org/10.1029/95JD01268, http://dx.doi.org/10.1029/95JD01268, 1995.

Barkstrom, B. R.: Some Effects of 8–12 μm Radiant Energy Transfer on the Mass and Heat Budgets of Cloud Droplets, Journal of the Atmospheric Sciences, 35, 665–673, https://doi.org/10.1175/1520-0469(1978)035<0665:SEORET>2.0.CO;2, http://dx.doi.org/10.1175/1520-0469(1978)035<0665:SEORET>2.0.CO;2, 1978.

Bott, A., Sievers, U., and Zdunkowski, W.: A Radiation Fog Model with a Detailed Treatment of the Interaction between Radiative Transfer and Fog Microphysics, Journal of the Atmospheric Sciences, 47, 2153–2166, https://doi.org/10.1175/1520-0469(1990)047<2153:ARFMWA>2.0.CO;2, http://dx.doi.org/10.1175/1520-0469(1990)047<2153:ARFMWA>2.0.CO;2, 1990.

Boucher, O., Randall, D., Artaxo, P., Bretherton, C., Feingold, G., Forster, P., Kerminen, V.-M., Kondo, Y., Liao, H., Lohmann, U., Rasch, P., Satheesh, S., Sherwood, S., Stevens, B., and Zhang, X.: Clouds and aerosols. In Climate Change 2013: The Physical Science Basis. Contribution of Working Group I to the Fifth Assessment Report of the Intergovernmental Panel on Climate Change., pp. 571–657, Cambridge University Press, 2013.

Brewster, M.: Evaporation and condensation of water mist/cloud droplets with thermal radiation, International Journal of Heat and Mass Transfer, 88, 695 – 712, https://doi.org/http://dx.doi.org/10.1016/j.ijheatmasstransfer.2015.03.055, http://www.sciencedirect.com/science/article/pii/S0017931015003130, 2015.

Caughey, S. J. and Kitchen, M.: Simultaneous measurements of the turbulent and microphysical structure of nocturnal stratocumulus cloud, Quarterly Journal of the Royal Meteorological Society, 110, 13–34, https://doi.org/10.1002/qj.49711046303, http://dx.doi.org/10.1002/qj.49711046303, 1984.

Cheng, W. Y. Y., Carrió, G. G., Cotton, W. R., and Saleeby, S. M.: Influence of cloud condensation and giant cloud condensation nuclei on the development of precipitating trade wind cumuli in a large eddy simulation, Journal of Geophysical Research: Atmospheres, 114, https://doi.org/10.1029/2008JD011011, https://agupubs.onlinelibrary.wiley.com/doi/abs/10.1029/2008JD011011, 2009.

Cooper, W. A.: Effects of Variable Droplet Growth Histories on Droplet Size Distributions. Part I: Theory, Journal of the Atmospheric Sciences, 46, 1301–1311, https://doi.org/10.1175/1520-0469(1989)046<1301:EOVDGH>2.0.CO;2, http://dx.doi.org/10.1175/1520-0469(1989)046<1301:EOVDGH>2.0.CO;2, 1989.

Davies, R.: Response of Cloud Supersaturation to Radiative Forcing, Journal of the Atmospheric Sciences, 42, 2820–2825, https://doi.org/10.1175/1520-0469(1985)042<2820:ROCSTR>2.0.CO;2, http://dx.doi.org/10.1175/1520-0469(1985)042<2820:ROCSTR>2.0.CO;2, 1985.

de Lozar, A. and Muessle, L.: Long-resident droplets at the stratocumulus top, Atmospheric Chemistry and Physics, 16, 6563–6576, https://doi.org/10.5194/acp-16-6563-2016, http://www.atmos-chem-phys.net/16/6563/2016/, 2016.

Feingold, G., (Tzitzvashvili), S. T., and Leviv, Z.: Evolution of Raindrop Spectra. Part I: Solution to the Stochastic Collection/Breakup Equation Using the Method of Moments, Journal of the Atmospheric Sciences, 45, 3387–3399, https://doi.org/10.1175/1520-0469(1988)045<3387:EORSPI>2.0.CO;2, https://doi.org/10.1175/1520-0469(1988)045<3387:EORSPI>2.0.CO;2, 1988.

Feingold, G., Walko, R., Stevens, B., and Cotton, W.: Simulations of marine stratocumulus using a new microphysical parameterization scheme, Atmospheric Research, 47, 505 – 528, https://doi.org/http://dx.doi.org/10.1016/S0169-8095(98)00058-1, http://www.sciencedirect.com/science/article/pii/S0169809598000581, 1998.

Feingold, G., Cotton, W. R., Kreidenweis, S. M., and Davis, J. T.: The Impact of Giant Cloud Condensation Nuclei on Drizzle Formation in Stratocumulus: Implications for Cloud Radiative Properties, Journal of the Atmospheric Sciences, 56, 4100–4117, https://doi.org/10.1175/1520-0469(1999)056<4100:TIOGCC>2.0.CO;2, https://doi.org/10.1175/1520-0469(1999)056<4100:TIOGCC>2.0.CO;2, 1999.

Grabowski, W. W. and Abade, G. C.: Broadening of Cloud Droplet Spectra through Eddy Hopping: Turbulent Adiabatic Parcel Simulations, Journal of the Atmospheric Sciences, 74, 1485–1493, https://doi.org/10.1175/JAS-D-17-0043.1, http://dx.doi.org/10.1175/JAS-D-17-0043.1, 2017.

Grabowski, W. W. and Wang, L.-P.: Growth of Cloud Droplets in a Turbulent Environment, Annual Review of Fluid Mechanics, pp. 293–324, https://doi.org/10.1146/annurev-fl-45-021013-200001, http://www.annualreviews.org/doi/abs/10.1146/annurev-fl-45-021013-200001, 2013.

Guan, H., Davies, R., and Yau, M.: Longwave radiative cooling rates in axially symmetric clouds, Journal of Geophysical Research: Atmospheres, 100, 3213–3220, 1995.

Guan, H., Yau, M., and Davies, R.: The Effects of Longwave Radiation in a Small Cumulus Cloud, Journal of the Atmospheric Sciences, 54, 2201–2214, 1997.

Guzzi, R. and Rizzi, R.: The effect of radiative exchange on the growth by condensation of a population of droplets, Beitraege zur Physik der Atmosphaere, 53, 351–365, 1980.

Harrington, J. Y., Feingold, G., and Cotton, W. R.: Radiative Impacts on the Growth of a Population of Drops within Simulated Summertime Arctic Stratus, Journal of the Atmospheric Sciences, 57, 766–785, https://doi.org/10.1175/1520-0469(2000)057<0766:RIOTGO>2.0.CO;2, http://dx.doi.org/10.1175/1520-0469(2000)057<0766:RIOTGO>2.0.CO;2, 2000.

Iacono, M. J., Mlawer, E. J., Clough, S. A., and Morcrette, J.-J.: Impact of an improved longwave radiation model, RRTM, on the energy budget and thermodynamic properties of the NCAR community climate model, CCM3, Journal of Geophysical Research: Atmospheres, 105, 14 873–14 890, https://doi.org/10.1029/2000JD900091, http://dx.doi.org/10.1029/2000JD900091, 2000.

Jiang, H., Feingold, G., and Sorooshian, A.: Effect of Aerosol on the Susceptibility and Efficiency of Precipitation in Warm Trade Cumulus Clouds, Journal of the Atmospheric Sciences, 67, 3525–3540, https://doi.org/10.1175/2010JAS3484.1, https://doi.org/10.1175/2010JAS3484.1, 2010.

Kablick, G., Ellingson, R., Takara, E., and Gu, J.: Longwave 3D Benchmarks for Inhomogeneous Clouds and Comparisons with Approximate Methods, Journal of Climate, 24, 2192–2205, 2011.

Khairoutdinov, M. F. and Randall, D. A.: Cloud Resolving Modeling of the ARM Summer 1997 IOP: Model Formulation, Results, Uncertainties, and Sensitivities, Journal of the Atmospheric Sciences, 60, 607–625, https://doi.org/10.1175/1520-0469(2003)060<0607:CRMOTA>2.0.CO;2, https://doi.org/10.1175/1520-0469(2003)060<0607:CRMOTA>2.0.CO;2, 2003.

Klinger, C. and Mayer, B.: Three-dimensional Monte Carlo calculation of atmospheric thermal heating rates , Journal of Quantitative Spectroscopy and Radiative Transfer, 144, 123 – 136, https://doi.org/http://dx.doi.org/10.1016/j.jqsrt.2014.04.009, 2014.

Klinger, C. and Mayer, B.: The Neighboring Column Approximation (NCA) –- A fast approach for the calculation of 3D thermal heating rates in cloud resolving models , Journal of Quantitative Spectroscopy and Radiative Transfer, 168, 17 –

28, https://doi.org/http://dx.doi.org/10.1016/j.jqsrt.2015.08.020, http://www.sciencedirect.com/science/article/pii/S0022407315002964, 2016.

Klinger, C., Mayer, B., Jakub, F., Zinner, T., Park, S.-B., and Gentine, P.: Effects of 3-D thermal radiation on the development of a shallow cumulus cloud field, Atmospheric Chemistry and Physics, 17, 5477–5500, https://doi.org/10.5194/acp-17-5477-2017, http://www.atmos-chem-phys.net/17/5477/2017/, 2017.

Köhler, H.: The nucleus in and the growth of hygroscopic droplets, Trans.Faraday Soc., 32, 1152 – 1161, 1936.

Langmuir, I.: THE PRODUCTION OF RAIN BY A CHAIN REACTION IN CUMULUS CLOUDS AT TEMPERATURES ABOVE FREEZING, Journal of Meteorology, 5, 175–192, https://doi.org/10.1175/1520-0469(1948)005<0175:TPORBA>2.0.CO;2, https://doi.org/10.1175/1520-0469(1948)005<0175:TPORBA>2.0.CO;2, 1948.

Lasher-Trapp, S. G., Cooper, W. A., and Blyth, A. M.: Broadening of droplet size distributions from entrainment and mixing in a cumulus cloud, Quarterly Journal of the Royal Meteorological Society, 131, 195–220, https://doi.org/10.1256/qj.03.199, http://dx.doi.org/10.1256/qj.03.199, 2005.

Lonitz, K., Stevens, B., Nuijens, L., Sant, V., Hirsch, L., and Seifert, A.: The Signature of Aerosols and Meteorology in Long-Term Cloud Radar Observations of Trade Wind Cumuli, Journal of the Atmospheric Sciences, 72, 4643–4659, https://doi.org/10.1175/JAS-D-14-0348.1, https://doi.org/10.1175/JAS-D-14-0348.1, 2015.

Mason, B.: The evolution of droplet spectra in stratus clouds, J. Meteor., 17, 459–462, 1960.

Mayer, B. and Madronich, S.: Actinic flux and photolysis in water droplets: Mie calculations and geometrical optics limit, Atmospheric Chemistry and Physics, 4, 2241–2250, https://doi.org/10.5194/acp-4-2241-2004, https://www.atmos-chem-phys.net/4/2241/2004/, 2004.

Mechem, D. B., Kogan, Y. L., Ovtchinnikov, M., Davis, A., Evans, K., and Ellingson, R.: Multi-Dimensional Longwave Forcing of Boundary Layer Cloud Systems, Journal of the Atmospheric Sciences, 65, 3963–3977, 2008.

Mlawer, E. J., Taubman, S. J., Brown, P. D., Iacono, M. J., and Clough, S. A.: Radiative transfer for inhomogeneous atmospheres: RRTM, a validated correlated-k model for the longwave, Journal of Geophysical Research: Atmospheres, 102, 16 663–16 682, https://doi.org/10.1029/97JD00237, http://dx.doi.org/10.1029/97JD00237, 1997.

Naumann, A. K. and Seifert, A.: Recirculation and growth of raindrops in simulated shallow cumulus, Journal of Advances in Modeling Earth Systems, 8, 520–537, https://doi.org/10.1002/2016MS000631, http://dx.doi.org/10.1002/2016MS000631, 2016.

Pruppacher, H. and Klett, J.: Microphysics of Clouds and Precipitation, Atmospheric and Oceanographic Sciences Library, Springer Netherlands, https://books.google.de/books?id=0MURkyjuoGMC, 2010.

Ramanathan, V., Cess, R. D., Harrison, E. F., Minnis, P., Barkstrom, B. R., Ahmad, E., and Hartmann, D.: Cloud-Radiative Forcing and Climate: Results from the Earth Radiation Budget Experiment, Science, 243, 57–63, https://doi.org/10.1126/science.243.4887.57, http://science.sciencemag.org/content/243/4887/57, 1989.

Roach, W. T.: On the effect of radiative exchange on the growth by condensation of a cloud or fog droplet, Quarterly Journal of the Royal Meteorological Society, 102, 361–372, https://doi.org/10.1002/qj.49710243207, http://dx.doi.org/10.1002/qj.49710243207, 1976.

Shaw, R. A., Reade, W. C., Collins, L. R., and Verlinde, J.: Preferential Concentration of Cloud Droplets by Turbulence: Effects on the Early Evolution of Cumulus Cloud Droplet Spectra, Journal of the Atmospheric Sciences, 55, 1965–1976, https://doi.org/10.1175/1520-0469(1998)055<1965:PCOCDB>2.0.CO;2, http://dx.doi.org/10.1175/1520-0469(1998)055<1965:PCOCDB>2.0.CO;2, 1998.

Simpson, G. C.: On the formation of cloud and rain, Quarterly Journal of the Royal Meteorological Society, 67, 99–133, https://doi.org/10.1002/qj.49706729002, http://dx.doi.org/10.1002/qj.49706729002, 1941.

Stephens, G. L.: Cloud Feedbacks in the Climate System: A Critical Review, Journal of Climate, 18, 237–273, https://doi.org/10.1175/JCLI-3243.1, http://dx.doi.org/10.1175/JCLI-3243.1, 2005.

Tzivion, S., Feingold, G., and Levin, Z.: An Efficient Numerical Solution to the Stochastic Collection Equation, Journal of the Atmospheric Sciences, 44, 3139–3149, https://doi.org/10.1175/1520-0469(1987)044<3139:AENSTT>2.0.CO;2, http://dx.doi.org/10.1175/1520-0469(1987)044<3139:AENSTT>2.0.CO;2, 1987.

Tzivion, S., Feingold, G., and Levin, Z.: The Evolution of Raindrop Spectra. Part II: Collisional Collection/Breakup and Evaporation in a Rainshaft, Journal of the Atmospheric Sciences, 46, 3312–3328, https://doi.org/10.1175/1520-0469(1989)046<3312:TEORSP>2.0.CO;2, http://dx.doi.org/10.1175/1520-0469(1989)046<3312:TEORSP>2.0.CO;2, 1989.

Črnivec, N. and Mayer, B.: Quantifying the bias of radiative heating rates in NWP models for shallow cumulus clouds, Atmospheric Chemistry and Physics Discussions, 2019, 1–28, https://doi.org/10.5194/acp-2018-1247, https://www.atmos-chem-phys-discuss.net/acp-2018-1247/, 2019.

Xue, H. and Feingold, G.: Large-Eddy Simulations of Trade Wind Cumuli: Investigation of Aerosol Indirect Effects, Journal of the Atmospheric Sciences, 63, 1605–1622, https://doi.org/10.1175/JAS3706.1, https://doi.org/10.1175/JAS3706.1, 2006.

Yamaguchi, T. and Randall, D. A.: Cooling of Entrained Parcels in a Large-Eddy Simulation, Journal of the Atmospheric Sciences, 69, 1118–1136, https://doi.org/10.1175/JAS-D-11-080.1, http://dx.doi.org/10.1175/JAS-D-11-080.1, 2012.

Zeng, X.: Modeling the Effect of Radiation on Warm Rain Initiation, Journal of Geophysical Research: Atmospheres, 123, 6896–6906, https://doi.org/10.1029/2018JD028354, https://agupubs.onlinelibrary.wiley.com/doi/abs/10.1029/2018JD028354, 2018.

Zhao, M. and Austin, P. H.: Life Cycle of Numerically Simulated Shallow Cumulus Clouds. Part I: Transport, Journal of the Atmospheric Sciences, 62, 1269–1290, https://doi.org/10.1175/JAS3414.1, https://doi.org/10.1175/JAS3414.1, 2005.